MICRO-PORE PARAMETRICS FOR OPTIMAL HYPERFILTRATION OF CONSERVATIVE CONTAMINANTS

A Thesis
Submitted to the Graduate Faculty
of the
North Dakota State University
of Agriculture and Applied Science

By

Anthony Walekhwa Wamono

In Partial Fulfillment
for the Degree of
MASTER OF SCIENCE

Major Program:
Environmental and Conservation Science

March 2012

Fargo, North Dakota

North Dakota State University
Graduate School

Micro-Pore Parametrics For Optimal Hyperfiltration Of

Conservative Contaminants

By

Anthony Walekhwa Wamono

The Supervisory Committee certifies that this ***disquisition*** complies with North Dakota State University's regulations and meets the accepted standards for the degree of

MASTER OF SCIENCE

SUPERVISORY COMMITTEE:

Dr. Peter Grala Oduor
Chair

Dr. Achintya Bezbaruah

Dr. Xinhua Jia

Dr. Wei Lin

Approved:

10/01/2012
Date

Dr. CRAIG STOCKWELL
Department Chair

ABSTRACT

In compacted Na-montmorillonite membranes, the pore-size, and surface charge will influence filtration processes of solutes. A dead-end hyperfiltration setup was utilized to: (a) study the intrinsic retention, membrane filtration coefficient, and solution flux of different membrane configurations and (b) model nitrate break-through effluent concentrations through the membrane. Scanning electron microscopy and solute analytical techniques were employed to assess what critical components of micro-pore parametrics would prevail in a non-bio stimulated remediation of simulated agricultural wastewater. Although high content bentonite membrane configurations (5 g clay at 2500 psi) offered better solute rejections with a 30 percent increase in the cell concentration, the compaction of the membrane had the most deterministic influence on the solution flux. The results reveal hyperfiltration of nitrate ions is a function of the compaction pressure and composition of bentonite in the mixed soils. High content bentonite membranes compacted at the optimal pressures offer promising solutions to nitrate contaminant remediation.

ACKNOWLEDGMENTS

I would like to thank my parents, Mr. James and Mary Wamono for believing in me and their numerous prayers, this is the foundation upon which everything has been built. I also extend my sincere gratitude to my advisor, Dr. Peter Oduor, for his mentorship, thoughtfulness and numerous suggestions. I would like to extend this gratitude to my thesis supervisory committee Drs. Achintya Bezbaruah, Xinhua Jia, and Wei Lin for insightful critiques.

I would to thank my colleagues Mohammad, Buddhika, Papia and Deidra their support. I express my heartfelt gratitude to Dr. Margaret Khaitsa and her family for making Fargo feel like home to me.

To God, who made completion of my studies possible.

TABLE OF CONTENTS

LIST OF TABLES

Table Page

LIST OF FIGURES

LIST OF SYMBOLS

Symbol	Description
ΔP	hydraulic pressure across the membrane
$\Delta\pi$	osmotic pressure across the membrane
D	unidirectional diffusion coefficient of solute in $cm^2 \cdot s^{-1}$
J_v	flux of solution directed toward high pressure side in $moles \cdot cm^{-2} \cdot s$
R	universal gas constant
J_s	flux of salt directed toward high pressure side in $moles \cdot cm^{-2} \cdot s^{-1}$
L_P	membrane filtration coefficient in $cm^2 \cdot s \cdot g^{-1}$
R_{int}	intrinsic retention value
x	position from high pressure side in cm
σ	the reflection coefficient (dimensionless)
$C_{(x,t)}$	transient state concentration of solute at any point in moles/liter
$C_{(o,t)}$	transient state concentration of solute entering membrane in moles/liter
$C_{(e,t)}$	effluent concentration of solute exiting membrane in moles/liter

LIST OF APPENDIX TABLES

1. INTRODUCTION

1.1. Conservative contaminants

A contaminant is a substance that is introduced in an environment where it does not belong in quantities that may have adverse effects on humans or the environment (Dorworth, 2003). Conservative contaminants are those that are permanent additions to the environment and not easily degradable (Cheung et al., 2011). Nitrate, which is soluble in water, may be considered to be conservative where advection is the main transport mechanism and significant attenuation is not possible due to its mobility. Also nitrate is relatively non-reactive in ground water and neither adsorbs to the aquifer matrix nor is consumed in an aquifer (Kasper, 2007). Nitrites and ammonia also contribute to nitrates in the environment since they are both oxidized to nitrates which remain stable in the environment (Krešić and Stevanović, 2010).

1.2. Sources and impacts of nitrate contamination

Contamination of ground and surface waters from agricultural waste is a significant challenge; many parts of the world report nitrate pollution as a key concern (Beeson and Cook, 2004; Burden, 1982; Rivett et al., 2007; Spalding et al., 1993). In the United States alone, about seventy percent of all ground water samples contain nitrate, moreover fifteen percent of these were in levels higher than set environmental protection agency (EPA) standards for potable water (Nolan and Stoner, 2000). Similarly in the developing world, the situation is not any better as the rate of nitrate pollution continues to rise as a result of increased application of nitrogen-based fertilizers (Okafor and Ogbonna, 2003; Zhang et al., 1996). In addition to agricultural sources; seepage of nitrates from septic tanks, lagoons and effluent discharge from waste treatment plants are the leading non-agricultural contributors of nitrate pollution (Munster, 2008).

The impact of nutrient enrichment due to nitrate contamination in water bodies is enormous; eutrophication, which is most visible, stands at the forefront of observable problems, but more subtle changes include the deterioration of the health of affected ecosystems (Dijk and de Groot, 1987; Griggs et al., 2003; Schäfer, 2012). Nutrient enrichment shifts the composition of the organisms in the ecosystem altering the competitive balance in the ecosystem (Nijboer and Verdonschot, 2004). Epidemiological studies have shown a negative association between elevated nitrate levels and the health of livestock (Fann et al., 1994).

Nitrate intake among humans occurs mainly by the ingestion of drinking water containing nitrates. When nitrates are consumed in elevated levels, they increase the risk of *methemoglobinemia*, a condition referred to as blue baby syndrome in infants (Fan and Steinberg, 1996). More effects of nitrate toxicity include carcinogenicity and hampering of thyroid functions (Gatseva and Argirova, 2008). In addition to the health risks associated with nitrate consumption, the socio-economic impacts from nitrate pollution include loss of tourism due to alteration of the recreational value of water bodies as a result of eutrophication. These alterations include odor and loss of visibility. Other economic impacts of nitrate pollution include lost revenue as a result of decreased fish harvest and increased costs of water treatment (Anderson et al., 2000, Ferreira et al., 2007). This makes nitrate contamination a very significant and widespread problem.

1.3. Nitrate removal techniques

Several nitrate removal techniques have been used in the drinking and wastewater treatment process with variable successes. Many water and wastewater treatment plants use biological processes to remove nitrates because of the low costs associated with them (Shrimali,

2000). Ion-exchange process, which is a another technique used in the drinking water purification removes nitrates and sulfates from water, is quite expensive and may inadvertently yield wastewaters with above regulatory limits of nitrates (Busch et al., 2005; De la Fuente García-Soto, 2005; Kabay, 2008). Hyperfiltration (also known as reverse osmosis or solute sieving) which is another wastewater remediation technique has the ability to remove smaller ions from solutions. Recently drinking water treatment works have adopted hyperfiltration technologies as a part of their water purification process (Redondo et al., 2003; Saffaj et al., 2004). Zero valent iron has been employed in permeable reactive barriers to treat ground water contaminated sites (Hashim et al., 2011). The zero valent iron is highly reactive at the nano scale, and quickly reduces the nitrates to nitrites and nitrogen (Shrimali, 2000). The down side to this process is the formation of oxides on the surface of the zero valent iron which slows the reduction process (Cheng et al., 1997; Rodríguez-Maroto, 2009; Westerhoff, 2003) and the increase in formation of ammonia which is an undesired byproduct (Hwang et al., 2011).

1.4. Hyperfiltration

Hyperfiltration is a membrane filtration process in which solute ions are retained on the high pressure side of the membrane while a more dilute solution exists on the lower pressure side (Fritz and Whitworth, 1994; Oduor, 2006). Hyperfiltration is dependent upon the application of a hydraulic gradient in excess of osmotic pressure across the membrane in the direction of water flow through the membrane (Whitworth, 1998). Because there is restriction of the flow of solute ions through the membrane, solute buildup on the high pressure end of the membrane results in a region known as a concentration polarization layer (CPL) (Fritz, 1986).

Hyperfiltration membranes have been used for water desalination as well as industrial separation processes (Merten, 1966; Wiesner, 1996; Rodríguez, 2001). Hyperfiltration is highly effective in the removal of both organic and inorganic compounds from water using natural or synthetic membranes (Huang et al., 1998; Weißbrodt et al., 2001). The recent research focus has been on the development of low pressure membranes with higher productivities (Peñate, 2012; Urairi, 1992). The process of hyperfiltration relies on maintaining initial flux rates, which tend to decline due to a process known as membrane fouling (Elimelech et al., 1997).

1.5. Membrane filtration processes

The membrane filtration process in the montmorillonite is governed by the interactions of charged solute ions and the surface charges on the membrane (Oduor et al., 2006). An electric field that spreads out beyond the edges of the clay particles is associated with Gouy layer (Oduor et al., 2009) in the double layers (see Figure 1). Under compaction, the Gouy layer adjacent to the clay platelet overlap (see Figure 2), creating a negatively charged field which restricts the movement of negatively charged solutes. (Coplen and Hanshaw, 1973; Hart et al., 2008).

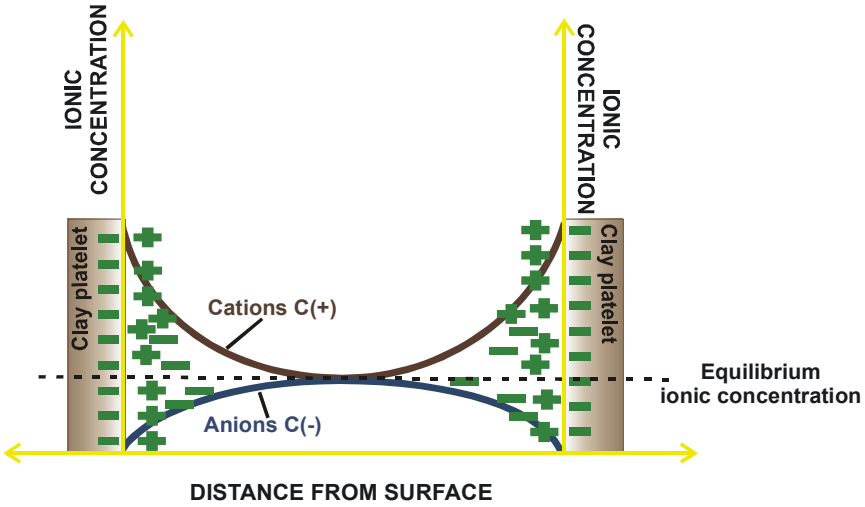

Figure 1. Electric double layer for adjacent clay platelets. The electrostatic potential decreases exponentially from the clay platelet (Oduor et al., 2009).

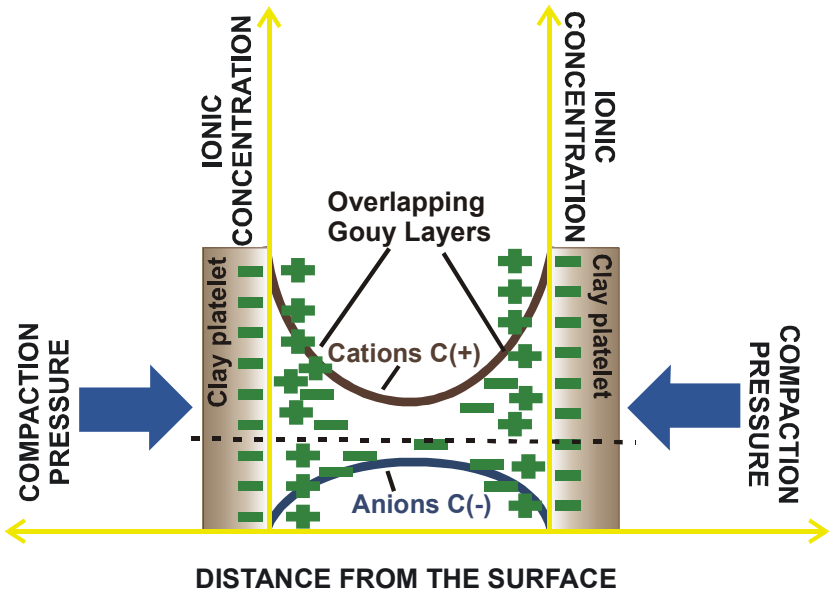

Figure 2. Distribution of ions under compaction. There is overlap of double layers under compaction (Oduor et al., 2009).

1.6. Theory

The negative surface charges and micron-sized pores and platelets in a compacted Na-montmorillonite membrane impede the transport of solute ions and, as a result, there is a buildup in the concentration of ions on the higher pressure side of the membrane (Fritz and Eady, 1985; Fritz and Marine, 1983; Fritz and Whitworth, 1994; Oduor et al., 2006). This induces electro-osmosis, thermo-osmosis, and chemical-osmosis due to the development of electrical, thermo, and concentration gradients respectively (Fritz and Eady, 1985; Fritz and Marine, 1983; Fritz and Whitworth, 1994; Oduor et al., 2006).

Hyperfiltration in imperfect semipermeable membranes occurs when the applied hydraulic gradient, ΔP, exceeds the realized osmotic pressure gradient, $\Delta\pi$, (Fritz and Eady, 1985; Fritz and Marine, 1983; Fritz and Whitworth, 1994; Oduor et al., 2006). The movement of ions as a result of a concentration gradient, $\partial C/\partial x$, in the direction of flow of solute results in the

development of a diffusive flux ($mol \cdot cm^{-2} \cdot s^{-1}$) (Fritz and Marine, 1983; Oduor et al., 2006; Oduor and Whitworth, 2004). The relationship between advective solution flux, J_v, the diffusion coefficient D, and the concentration C, at any point of interest is given by (Fritz and Marine, 1983; Oduor et al., 2005):

$$\left(\frac{\partial C}{\partial t}\right) = -J_v\left(\frac{\partial C}{\partial x}\right) - D\left(\frac{\partial^2 C}{\partial x^2}\right) \tag{1}$$

An increase in concentration of the ions, for example nitrate ions, adjacent to the membrane on the high pressure side as a result of hyperfiltration increases the resistance to flow of subsequent nitrate ions advected towards the membrane. Thus, a back-diffusion $J_d = -D\partial C / \partial x$ due to the concentration gradient arises. The hydraulic gradient that drives nitrate ions in the direction of flow across the membrane gives rises to a solute flux J_s, ($J_s = C_x J_v$) (Fritz and Marine, 1983; Oduor et al., 2006; Oduor and Whitworth, 2004). The solution to Equation (1) for the following boundary conditions $C(0,t) = C_{(0,t)}$ for $t \leq 0$; $C(x, 0) = 0$ for $x \leq 0$; $C(\infty, t) = 0$ for $t \leq 0$ (Oduor et al., 2006; Oduor and Whitworth, 2004) is

$$C_{(x,t)} = \left[\frac{C_i}{2}\right]\left\{\left[\exp\left(\frac{-J_v x}{D}\right) - 1\right]\operatorname{erfc}\left(\frac{x - J_v t}{2(Dt)^{1/2}}\right) + \operatorname{erfc}\left(\frac{x + J_v t}{2(Dt)^{1/2}}\right)\right\} + C_i, \tag{2}$$

where t is time in seconds and C_i the initial concentration. The advective solution flux is governed by

$$J_v = L_P\left(\Delta P - \sum_{i=1}^{n} \sigma_i \Delta\pi_i\right), \tag{3}$$

where ΔP is the transmembrane pressure, L_p is the hydraulic permeability of a membrane, σ_i is the membrane efficiency for solute i, and $\Delta\pi_i$ is the theoretical osmotic pressure existing across

the membrane as a result of solute ions *i* (Oduor and Whitworth, 2005). The osmotic pressure is derived from the concentration gradient according to (Oduor, 2004):

$$\Delta\pi = \upsilon RT\Delta C, \tag{4}$$

where υ is the number of constituent ions, R is the universal gas constant with a value of 8.314 $J\cdot mol^{-1o}K^{-1}$, T is the absolute temperature in Kelvin, and ΔC is the concentration gradient in $mol\cdot l^{-1}$.The Concentration Polarization Layer (CPL) is a manifestation of solute buildup where C_o, concentration adjacent to the membrane, is higher than the influent concentration, C_i on the influent side (Figure 3) (Fritz and Whitworth, 1994; Oduor and Whitworth, 2005). For a membrane of thickness $\Delta x = x$ *cm,* subjected to a solution flux (J_v in $cm\cdot s^{-1}$), the advection of the solute ions towards the membrane is governed by the relation $J_s = C_x J_v$, where C_x is the concentration at a distance x (see Figure 3) (Oduor et al., 2009).

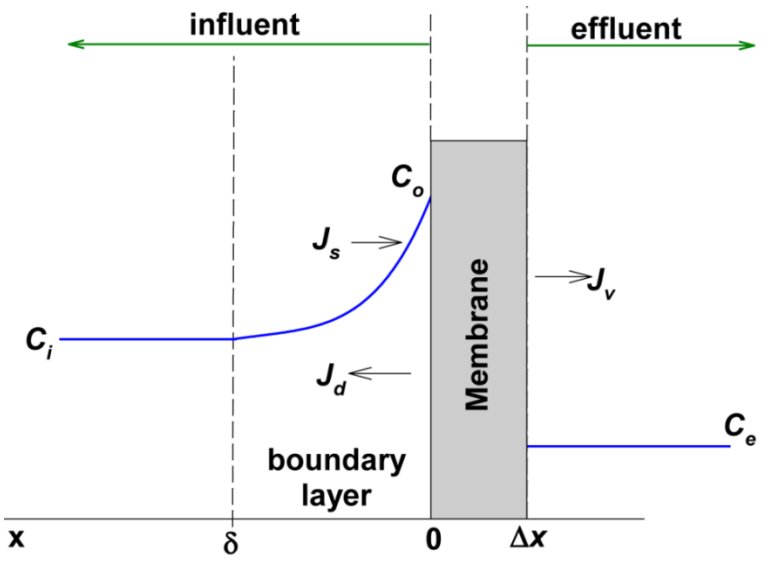

Figure 3. Illustration of concentration profile (redrawn from Oduor et al., 2009).

Oduor et al. (2009) related the solute rejection in a non-ideal membrane, such as geo-membranes, in a closed system as in Fig. 3 to:

$$C_x J_v + D\frac{dC}{dx} = C_e J_v . \tag{5}$$

The integration of Equation (5) at boundary conditions $C_x = C_o$ where $x = 0$ and steady state $C_x = C_i$ where $x = \delta$, results in (Oduor et al., 2009):

$$\left(C_0 - C_e\right) = \left(C_i - C_e\right)\exp\left(\frac{J_v}{q}\right), \tag{6}$$

where $q = \left(D/\delta\right)$ is the mass transfer coefficient in $\text{cm}\cdot\text{s}^{-1}$.

The dimensionless intrinsic retention R_{int} is given by (Mulder, 1995; Oduor and Whitworth, 2005):

$$R_{\text{int}} = \left[1 - \frac{C_e}{C_0}\right]. \tag{7}$$

The intrinsic retention can be used as an approximation of reflection coefficient assuming that isothermal conditions prevail, the density of solution remains constant , and an isotropic media exists (Oduor et al., 2005, 2004). Reflection coefficients characterize the ease with which membranes admit water ions in preference to solute ions (Oduor, 2004). The membrane efficiency, as represented by the reflection coefficient, is a function of the filtration coefficient (Oduor and Whitworth, 2005). The solution (Fritz and Marine, 1983) to the advection-diffusion Equation (1) for a type-one Dirichlet boundary condition with a constant influent concentration C_i, and $C_0 = C_i$ is (Oduor and Whitworth, 2005):

$$\frac{C_x}{C_i} = \frac{1}{2}\left(\text{erfc}\left[\frac{(x - J_v t)}{\sqrt{4Dt}} \right] + \exp\left\{ \frac{J_v x}{D} \right\} \text{erfc}\left[\frac{(x + J_v t)}{\sqrt{4Dt}} \right] \right), \tag{8}$$

where $x = \Delta x$ (thickness of the membrane), $C_{(x,t)}$ is the transient concentration and $C_{(e,t)}$ is the effluent concentration. The solution flux, J_v at a given time t can be derived from experimental data (Oduor et al., 2006, Oduor and Whitworth, 2005). The $\text{erfc}\left((x - J_v t)/\sqrt{4Dt}\right)$ term of Equation (8) becomes the dominant transport process since $\exp\{J_v x/D\}\text{erfc}\left((x + J_v t)/\sqrt{4Dt}\right)$ approaches zero for steady state solution flux. Equation (8) can be reduced to (Oduor et al., 2006):

$$2\left(\frac{C_e}{C_i}\right) = \text{erfc}\left[\frac{\Delta x - J_v t}{\sqrt{4Dt}} \right], \tag{9}$$

with an accuracy limited to the third decimal place.

The concentration on the high pressure side of the membrane $C_{(0,t)}$ is given by one-dimensional transport equation (Oduor et al., 2006):

$$\text{C}_{(0,\,t)} = \begin{cases} C_i & \text{for} \quad t = 0 \\ \left[\frac{C_i}{2}\right]\left\{\left[1 + \text{erf}\left(\frac{J_v^{\,2} t}{4D}\right)\right]\right\} + C_i & \text{for} \quad t > 0 \end{cases}. \tag{10}$$

With known values of solution flux at steady state and influent concentrations, the break-through effluent concentrations $C_{(e,t)}$ can be modeled using (Oduor et al., 2006):

$$C_{e(t)} = C_i - \left[C_{(0,t)} \left(1 - \exp\left(\frac{J_v \Delta x}{2D} \right) \left(1 - \sqrt{\left(1 + \frac{8D}{(J_v)^2 t} \right)} \right) \right) \right]. \tag{11}$$

With solution flux calculated, membrane filtration coefficient can be obtained empirically using Equation (3) (see appendix Tables A1, A2, A3). Equation (10) can be used to model the development of the nitrate concentration $C_{(0,t)}$ in the CPL a necessary parameter needed to model the effluent concentration across the membrane (see also appendix Tables A1, A2, A3). The modeled break-through effluent concentrations using Equation (11) and the empirically derived concentrations can then be compared.

1.7. Objectives

The main objective of the study presented in this thesis was:

To study (a) the influence of the percentage of clay in a clay–glass bead mixture and (b) compaction of clay–glass bead mixture on hyperfiltration of a nitrate solution.

1.8. Hypothesis

Membrane efficiency will increase with higher compaction pressures and percentage of Na-montmorillonite in the clay-glass-beads mixture.

1.9. Organization of thesis

This document presents the findings of the study carried out to investigate the influence of micropore parameters on the hyperfiltration of nitrate ions. The thesis starts with an introductory chapter 1, followed by literature review in chapter 2. The materials and methods adopted for the experiments are described in chapter 3. The results and discussion are in chapter 4 while a summary of the conclusions is in chapter 5. References and appendices are included at the end of the thesis.

2. LITERATURE REVIEW

2.1. Clay and clay minerals

Soil types can be grouped into gravel, sand, loam, silt, and clays. Where the classification is based on grain size, then clay soils can be simply defined as fine grains whose diameter is less than 2 μm (Filgueira, 2006). Clay minerals can be also defined as phyllosilicates formed through chemical weathering of silicate minerals of the earth's surface (Zhang, 2010). The difference between clay and clay minerals is that clay is made of one type of mineral whereas clay minerals are made of more than just one type of clay (Bergaya and Lagaly, 2006). Clay minerals can be formed into tetrahedron and octahedron sheet structures (Birkeland, 1999). The difference between these two sheets lies in the geometric arrangement of the particular cations (silicon, aluminum, magnesium, iron) and anions (oxygen and hydroxide) that make the structure (Figure 4). The clay minerals are classified into seven groups (1) kaolin-serpentine, (2) pyrophyllite-talc, (3) smectite, (4) vermiculite, (5) mica, (6) chlorite, (7) interstratified clay minerals (Zhang, 2010 one more). This classification is done on the basis of the net layer charge per formula unit, characteristic of layer type, interlayer species as shown in Table 2.1 (Martin et al., 1991; Zhang, 2010).

2.2. Smectites

Smectites group of clay minerals are comprised of a succession of dioctahedral or trioctahedral layers (Figure 4) having a geometric structure where the inter layer spacing is filled with exchangeable cations and water in the ratio of 2:1 (Guichet, 2008). Na-montmorillonite is a form of smectites where the Na^+ ions form of the smectites varies the amount of interlayer water and has a high cation exchange capacity, and a high surface charge (K) (Heister, 2005).

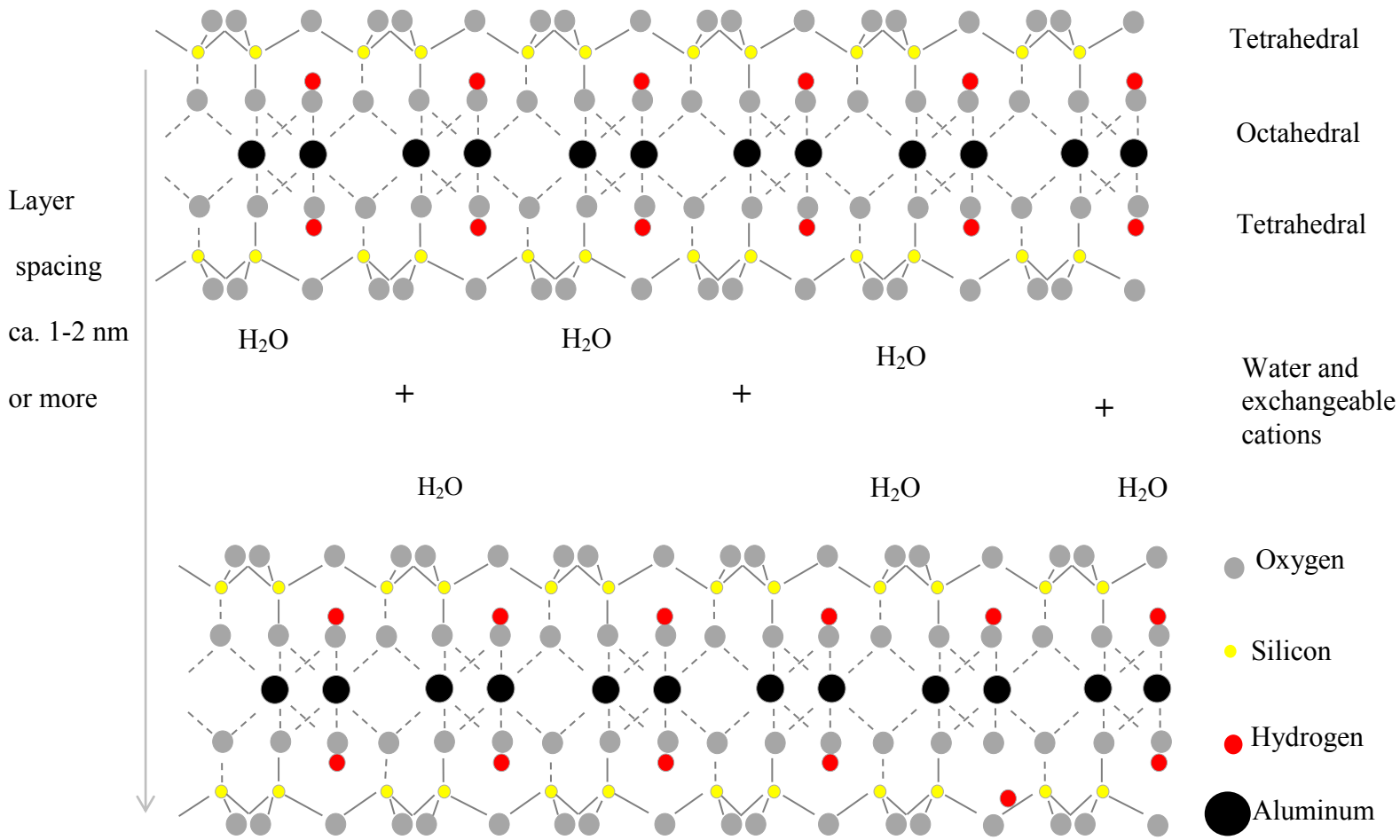

Figure 4. Structure of montmorillonite (redrawn from Schmidt et al., 2005).

Table 1. Classification of clay minerals (Zhang, 2010).

Layer type	**Interlayer material**	**Group**		**Species**
1:1	None or H_2O only	Kaolin–serpentine	Trioctahedral	Lizardite, berthierine, amesite, cronstedtite, nepouite, kellyite, fraipontite, brindleyite
	(x～0)		Dioctahedral	Kaolinite, dickite, nacrite, halloysite (planar)
			Di-triotahedral	Odinite
2:1	None	Pyrophyllite-Talc	Trioctahedral	Talc, willemseite, kerolite, pimelite
	(x～0)		Dioctahedral	Pyrophyllite, ferripyrophyllite
	Hydrated exchangeable cations	Smectite	Trioctahedral	Saponite, hetorite, sauconite, stevensite, swinefordite
	(x～0.2–0.6)		Dioctahedral	montmorillonite, beidellite, nontronite, volkonskoite
	Hydrated exchangeable cations	Vermiculite	Trioctahedral	Trioctahedral vermiculite
	(x～0.6–0.9)		Dioctahedral	Dioctahedral vermiculite
	Non-hydrated monovalent cations	True (flexible) mica	Trioctahedral	Biotite, phlogopite, lepidolite, etc.
	x～0.6–1.0)		Dioctahedral	Muscovite, illite, glauconite, celadonite, paragonite, etc.
	Non-hydrated divalent cations	Brittle mica	Trioctahedral	Clintonite, kinoshitalite, bityite, anandite
	(x～1.8–2.0)		Dioctahedral	Margarite
	Hydroxide sheet	Chlorite	Trioctahedral	Clinochlore, chamosite, pennantite, nimite, baileychlore
	(x = variable)		Dioctahedral	Donbassite
			Di-triotahedral	Cookeite, sudoite
2:1	Regularly interstratified	Variable	Trioctahedral	Corrensite, aliettite, hydrobiotite, kulkeite
	(x = variable)		Dioctahedral	Rectorite, tosudite

The cation exchange capacity is defined as the total number of cations absorbed at a given pH (Favre et al., 2002, 2006; Rhoades, 1982; Stucki et al., 1997). The high surface charge and high cation exchange capacity of smectites make these clays the best option for use in waste containment structures (Shen et al., 1992).

2.3. Membrane fouling

Membrane fouling may be defined as the process by which solute ions or molecules are retained at the surface of the membrane or inside the pore wall leading to a decline in the flux of the membrane (Mulder, 1996; Shirazi et al., 2010). The effects of membrane fouling are manifested by reduction in the permeate flux resulting in a decrease in membrane efficiency (Saffaj et al., 2004; Shirazi et al., 2010). The process of fouling in membranes during hyperfiltration and other pressure driven filtration systems can be attributed to: (a) decrease of the hydraulic gradient as result of osmotic pressure (Probstein et al., 1981); (b) development of concentration polarization boundary layer which offers resistance to flow of macromolecules (Goldsmith and Lolachi, 1970; Oduor et al.,2005) (c) plugging of the pores in the membrane, reducing the flow paths of the macromolecules (Oduor et al., 2005; Shaalan et al., 2002;); and (d) resistance of an adsorption layer (Mulder, 1995; Oduor, 2005; Shirazi et al., 2006). The physico-chemical interactions of the solute ions and the surface of the membrane, for example, hydrophobic interactions, molecule polarization, and hydrogen bonding through charge transfer result in the adsorption of molecules to the membrane surface (Mulder, 1995).

2.4. Membrane filtration mechanisms

The membrane behavior of porous media which restricts the migration of solutes in clays or soils with clay materials is an established phenomenon (Berry, 1967; Kharaka and Berry,

1974; Fritz, 1983 and 1987; Oduor et al., 2006; Srivastava et al., 1975). This results in chemico-osmosis or the flow of liquid in response to a chemical concentration gradient **(**Graf, 1982; Keijzer, 2000; Kooi et al., 2003). Numerous studies have reported the existence of membrane behavior in bentonite based hydraulic barriers commonly used in waste containment applications (Kang et al., 2006). Homo-ionic clays like Na-montmorillonite under mechanical compaction act as an imperfect ion exclusion membrane because of their surficial negative charges, micron sized platelets, and attendant small pores (Oduor et al., 2006). As a result of the membrane behavior in compacted clays like Na-montmorillonite, the CPL starts from the membrane surface on the high pressure side and extends on the high pressure side until it levels out with the influent concentration (Fritz, 1994; Mulder, 1995; Oduor et al., 2009; Strathmann, 1968; Wijmans, 1985). The influence of the CPL on the efficiency of the membrane is a result of ions competing for exchange sites, back diffusive flux from the rejected solutes by the membrane, and ionic transport resistance within the membrane (Oduor et al., 2009).

Oduor et al. (2009) deduced that as long as the permselectivity of a homo-ionic membrane like Na-montimorillonite remains constant, the plugging of the pores at ultra -high hydraulic gradients shows non-uniform trends. Using maximal hydraulic pressure and the average osmotic pressure, their study profiled mass transfer coefficient within the first 10 days into five phases as shown in Figure 5.

In the Hart et al. (2008) study, membrane behavior in Kaolinite which is a clay mineral with less membrane properties than Na-montimorillonite was evaluated. Membrane behavior was reported to occur at pressures lower than were previously thought. Three low head hyperfiltration experiments were conducted using dilute solutions of chloride ions (Cl^-) in a

hyperfiltration cell, the increase in the cell concentration of Cl^- indicated the occurrence of solute sieving (hyperfiltration).

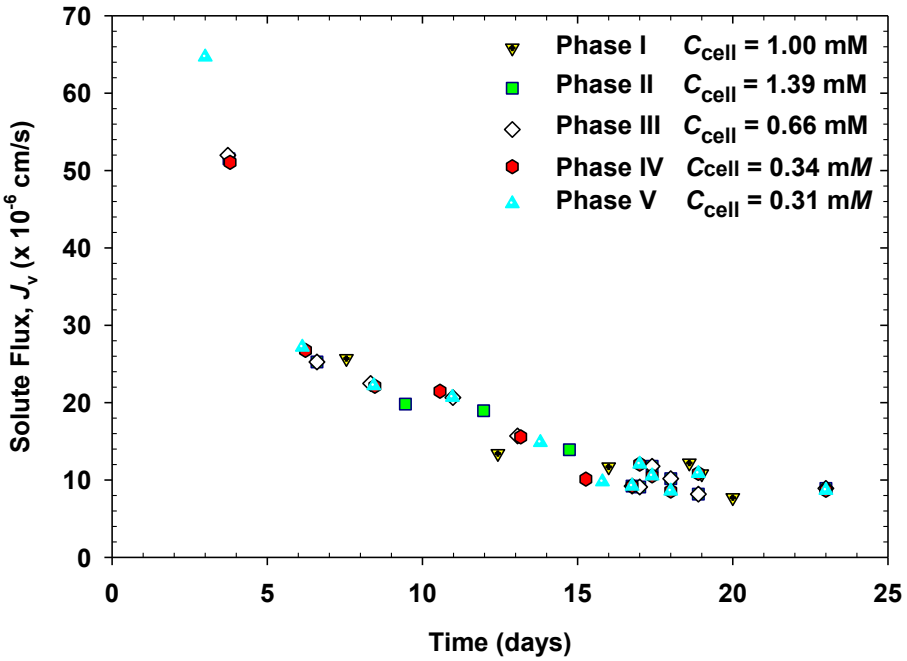

Figure 5. Solute flux variation for different hydraulic pulse phases (Oduor et al., 2009).

This increase in concentration has significant implications on the subsurface processes such as fate and transports of contaminants, subsurface microbiology, and natural attenuation among others (Hart et al., 2008). Derrington et al. (2006) found nitrate cell concentrations of up to 1.55 times greater than initial concentrations and calculated values of reflection coefficient range of 0.58 to 0.084 for low hydraulic gradient systems. The pressure gradients used were similar to those in shallow clay lined engineered systems like earthen lagoons for agricultural waste (Derrington et al., 2006; Metcalf and Eddy, 2003).

In a laboratory setting, glass beads mixed with clay have been used to simulate mixed soils in nature where the glass beads represent sand-sized particles (Abichou et al., 2002).

Saindon et al. (2006) varied the composition of glass beads/clay ratio starting from 100% clay to 100% glass beads to make membrane samples that were subject to compaction. The concentrations in both the permeate and concentrate were measured. The hydraulic conductivity and rejection coefficient were obtained as a basis for establishing the membrane behavior. The results reveal that membrane behavior is exhibited with as low as 12% clay- glass beads ratio (Sandon et al., 2006). Ishiguro et al. (1995) used a 0.5 mm thickness montmorillonite membrane, which was sandwiched between Millipore® filter papers, and used in hyperfiltration experiments for various inorganic and organic solutes. The effectiveness of membrane separation of solute was noticed to be highest using very low molar concentrations of sodium chloride and a negatively charged membrane.

Liangxiong et al. (2003) investigated the possibility of purifying oil-field produced water using a bentonite clay membrane by determining the inorganic solute rejection capabilities of the membrane when subject to a solution with multiple similar anions. Four different dilutions were used as feed solutions, while keeping the other operational conditions of pressure, temperature and flow rate constant. The analysis of the permeate indicated that solute rejection by the bentonite membrane decreased with increasing ionic concentration and decreased with increasing total dissolved solids (TDS). The anion rejection of the SO_4^{2-} was greater than that of Cl^- where the multivalent ions had a higher rejection. Liangxiong et al. (2003) concluded that the prediction of solute rejection sequences for multi-component waters similar to oil-field produced water is not clear-cut especially for the cations.

2.5. Hyperfiltration using Geomembranes

Many waste containment structures, for example slurry walls and Geosynthetic Clay Liners (GCL) with membrane properties are made of clay mixed with other soil particles and other materials (Yoo et al., 2009). GCLs have been used to attenuate the concentration of metals from lime treated mine tailings while maintaining a neutral pH and low hydraulic conductivity (Lange et al., 2010). Kang and Shackelford (2009) tested the membrane behavior of geosynthetic clay liner containing sodium bentonite. A flexible-wall cell was developed to measure the membrane behavior of clay soils in a closed–system. In their experimental setup, they tested consolidated membrane in multiple stages by establishing the pressure difference between the top and bottom cell. De-ionized water was circulated across both the bottom and top of the cells to establish the baseline pressure difference. This was followed by circulation of different concentrations of potassium chloride (KCl) solutions across the top of the specimen, while maintaining the circulation of de-ionized water at the bottom. The results show that membrane efficiencies obtained in a flexible are similar to those in a rigid cell.

2.6. Negative rejection

Negative rejection, a phenomenon where the solute ions are more concentrated in the permeate than in the feed solution, although rarely observed has been reported (Tsuru et al., 1991; Bardot et al., 1995). Although this has been exhibited in cross-flow configurations, there may be likelihood that it is an effect that can be observed in dead-end hyperfiltration. Utilizing elements of negative cation rejection, Jiang et al. (2003) evaluated a pore filled cation exchange membrane in pressure-driven separation of inorganic salts. Using low pressure membranes, the separation performance of single solute was dependent on salt concentration, and the

performance of mixed solutes was dependent on concentration and concentration ratio as seen in the graphs shown below (Figures 6) (Jiang et al., 2003).

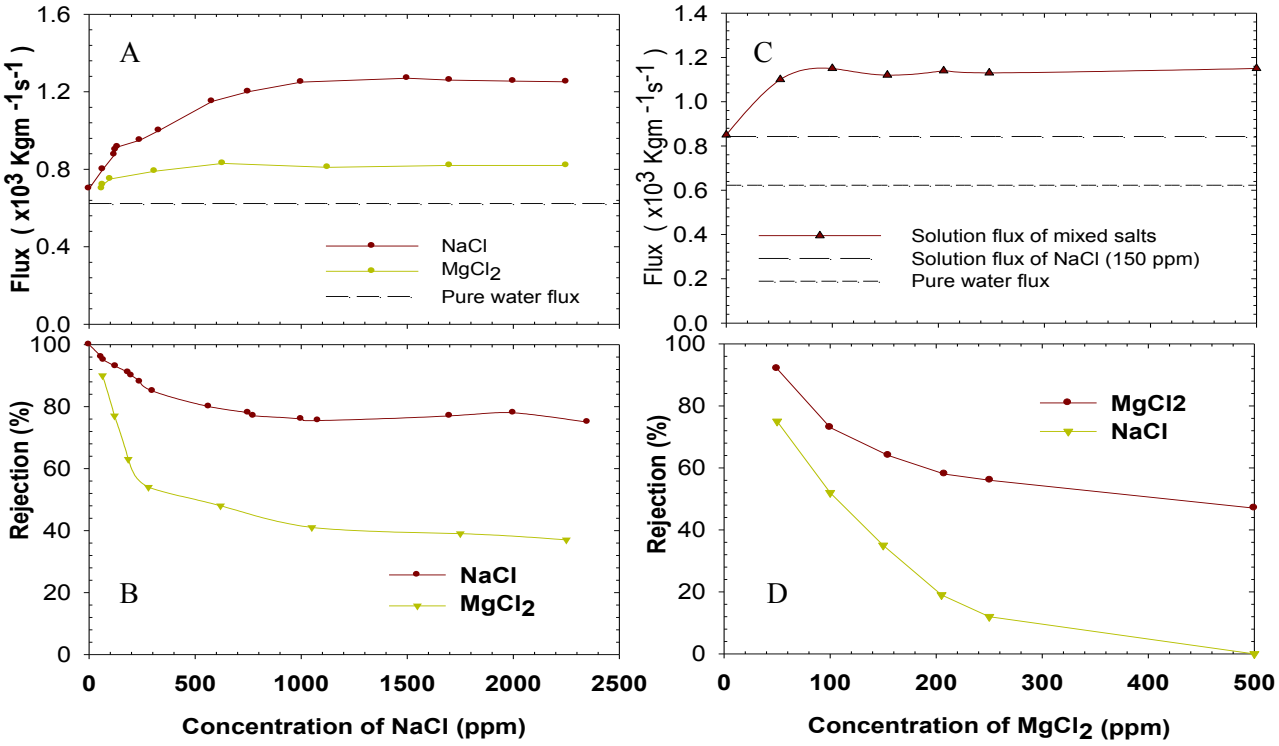

Figure 6. (A) and (B) Membrane efficiency in mixed salt system (Jiang et al., 2003), (C) and (D) show membrane efficiency in a single salt system (Jiang et al., 2003).

Polyelectrolyte gels are cation-exchange membranes containing poly (styrene-divinylbenzene sulfonic acid) filled in a polyethylene membrane which can be used in nanofiltration and as well as in hyperfiltration systems (Jiang et al., 2003). In a membrane system having bivalent ions, the effect of charge screening is higher compared to the monovalent counter-ions (for example Na^+), the interaction of the bivalent counter-ions (for example Mg^{2+}) in the membrane is with two fixed charges, which results in "ionic cross linking" (Jiang, 2003).

3. MATERIALS AND METHODS

3.1. Experimental setup

The powdered bentonite used was SWy-1 Na-montmorillonite from Crook County, Wyo (Dept. of Geology, University of Missouri, Columbia, Missouri USA) (for example Oduor et al., 2009). Dried samples of the Na-montmorillonite (clay) were mixed with glass beads (Ferro Corporation®, item 2332.5) to form different configurations of the membrane. The pure configuration consisted of 5 g clay, and the other configuration consisted of a mixture of 5 g clay and 10 g glass beads. Both configurations were mixed with 40 ml of deionized water in a beaker using a stirrer until a uniform slurry was obtained. The resulting mixture was poured into a stainless steel tube attached to an stainless steel cylinder with one end closed by a porous stone frit, Whatman® filter paper and a 0.1 µm Millipore® membrane (Figure 7).

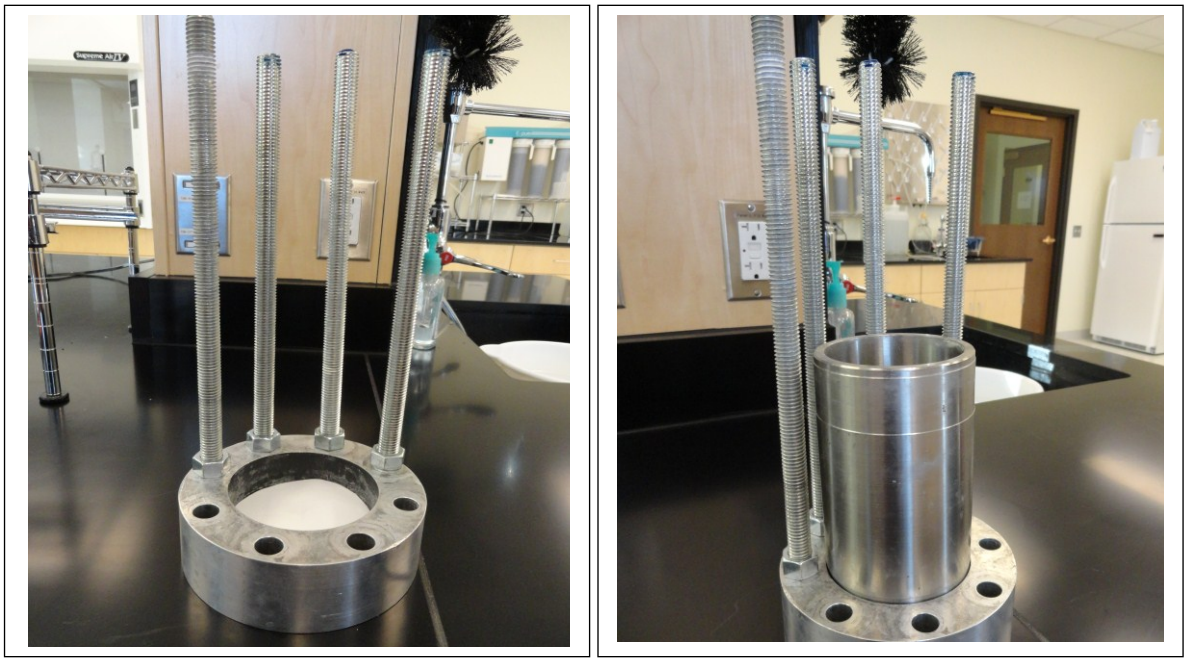

Figure 7. Stainless steel cylinder with one end closed by a porous stone frit (right).

The top part of the stainless steel tube was attached to a stainless steel cap. The entire assembly (Figure 8) formed a high-pressure dead-end filtration cell as described in Oduor et al., (2009).

Figure 8. Photograph of the dead-end hyperfiltration cell assembly.

The compaction of the membrane was accomplished by forcing deionized water through the membrane. The membranes were compacted at differential pressures of 500 psi and 2500 psi. To examine the effects of higher pressure, a separate experiment was set for 5 g clay and 10 g glass beads at 4500 psi. Control experiments were performed prior to each membrane experiment using deionized water and nitrate solution through membranes containing only glass beads, 0.1 μm filter paper. The main experimental set up is as shown in Figures 9 and 10.

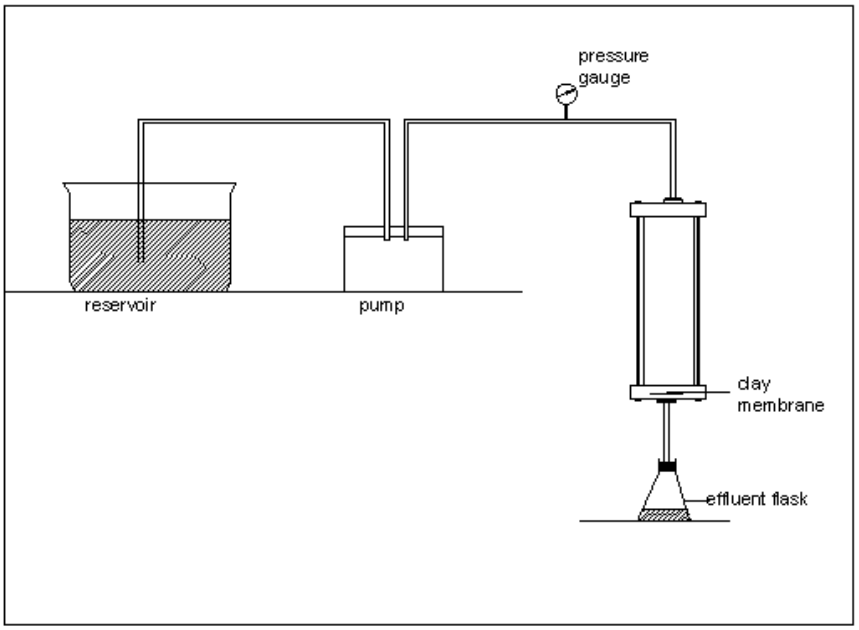

Figure 9. Schematic diagram of the experimental

Figure 10. Photograph showing the experimental setup.

The clay-glass beads mixture was compacted using a Millipore HPLC pump (Waters model 510: Figure 11) able to withstand a maximum back-pressure of 6,000 psi by passing

deionized water. In the low pressure system, a pump able to withstand a back-pressure of 500 psi was used to compact the clay-glass beads mixture. The rest of the procedures were identical to the high pressure system aforementioned. The deionized water was replaced with a nitrate solution made by dissolving analytical grade sodium nitrate in deionized water and inflow rate was set to 0.1 ml/min. There was a steady increase of hydraulic pressure until a steady pressure was achieved for the high pressure system. There was not any measurable pressure build up in the low pressure system.

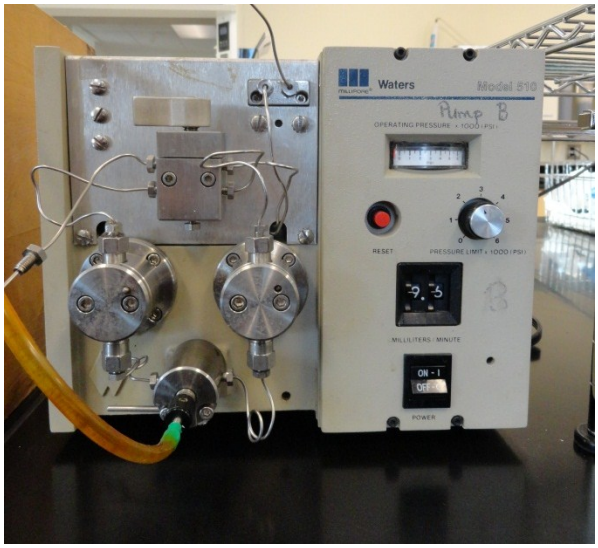

Figure 11. Photograph of Millipore HPLC pump Waters model 510.

Effluent samples were collected in 150 ml capped sampling bottles for analysis over measured time intervals and the solution flux was calculated using (Oduor et al., 2009):

$$J_v = Q/A. \tag{12}$$

After the experiment, the average membrane thickness and area were carefully measured.

3.2. Scanning Electron Microscopy

Samples for Scanning Electron Microscopy (SEM) were prepared by slow evaporation of the clay glass-bead membrane on glass slides and petri-dishes. SEM imagery was used to determine the range for glass bead radii and to look at the surface morphology of the membranes. A portion of about 1 cm^2 of the clay on the filter-paper substrate was cut out with a razor blade and allowed to air dry at room temperature overnight. The dried section was adhered to a cylindrical aluminum mount with silver paste. A conductive gold-palladium layer was applied to the surface using a sputter coater (SCD 030, Balzers, Liechtenstein). Specimens were observed and imaged at 15 kV with a JEOL JSM-6490LV scanning electron microscope (JEOL USA, Peabody, MA).

3.3. Chemical analysis

The chemical analysis involved testing ultra-high purity water, de-ionized water, and various standard nitrate control concentrations along with the effluent samples. This was done using a Dionex Ion Chromatograph 2000 (ICS, 2000) System (Figure 12). The ICS 2000 system requires priming of the pump for 15 to 20 minutes followed by the creation of a program, method and sequence setup that involves particular settings for the analysis of the samples.

The ICS 2000 system parameters support an EluGen KOH cartridge which is programmed to generate a potassium hydroxide eluent concentration of 23.0 mM, an operating temperature of 30° C, an injection volume of 20 µl and an anion atlas electrolytic suppressor that detects the analytes. All the samples were transferred into 5 ml vials, filled to marked lines and capped with filter caps to prevent evaporation, contamination and spillage during analysis. The filled vials were placed into cassettes, holding six vials each. Samples were loaded based on a

prescribed sequence. The first three samples in the analysis were MilliQ water (ultra-high purity water) followed by three vials containing deionized water. Ultrahigh purity water was used to flush out detritus ions in the ICS 2000 and to provide a safe analysis buffer since the chromatograms of the first few samples may deviate as the system calibrates itself. Subsequent vials included several standards consisting of sodium nitrate solutions, and 18-30 effluent samples. All the samples were loaded automatically and injected through an AS40 auto-sampler. Ultrahigh purity helium gas was used to stabilize the system background pressure. All samples were analyzed in triplicate and an average concentration used. Nitrate peaks were considered if they occurred within the specification window of ± 0.535 minutes, thus the range was 9.715 minutes to 10.785 minutes. Both the retention and peak precision times of the nitrate anion were determined based on the U.S. EPA Method 300 (for example Cheshire et al., 1983).

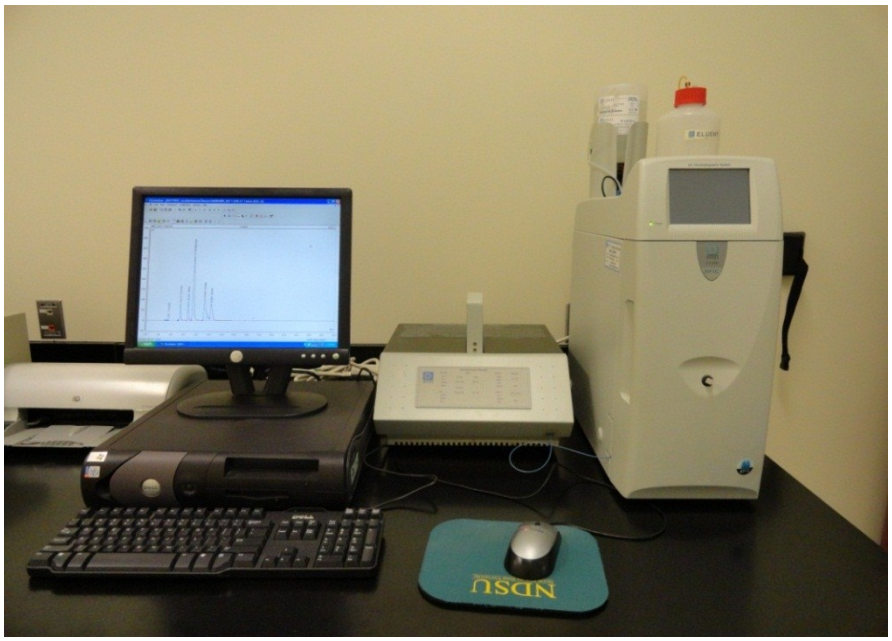

Figure 12. Photograph of the Dionex ICS 2000 Ion Chromatograph.

4. RESULTS AND DISCUSSIONS

4.1. Scanning electron microscopy

Samples of air dried membranes were imaged using s scanning electron microscope (SEM). Images displayed in the Figure (13) show the random orientation of the clay platelets in forming a membrane. SEM of the 5 g clay membrane shows a well formed surface with irregularly shaped flaky smectites particle edges of different sizes.

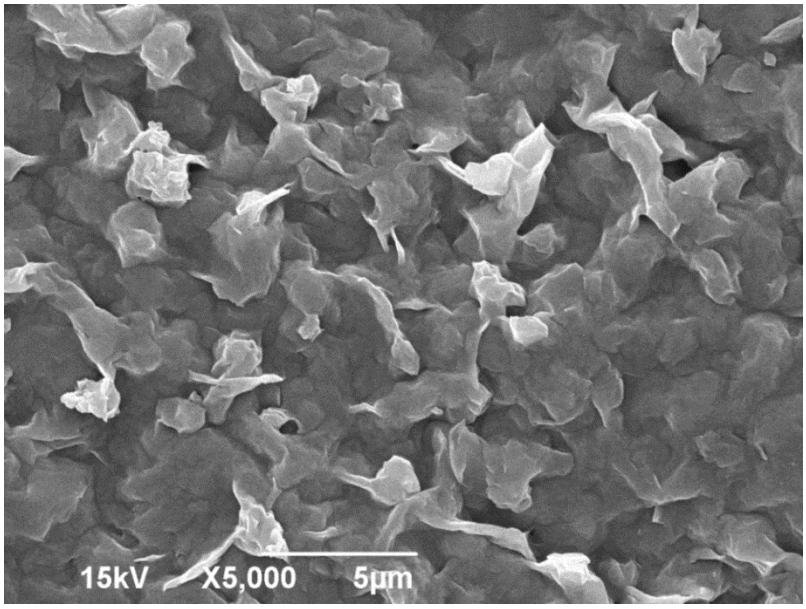

Figure 13. Scanning electron microscope image of 5 g clay membrane after hyperfiltration.

In the membrane formed from the 5 g clay and 10 g glass beads, the SEM reveals a uniform distribution of the glass bead and clay (Figure 14); this implies that preferential paths for solution to follow were minimized. SEM techniques were important in characterizing the size of the glass beads used in making the different configurations of membranes (Figure 15). From the average particle size, it is accurate to state that the glass beads are representative of silt and fine

sand sized particles. Most naturally occurring bentonites used in environmental containment structures are comprised of Na-montmorillonite mixed with fine grained sand particles (Yoo et al., 2009).

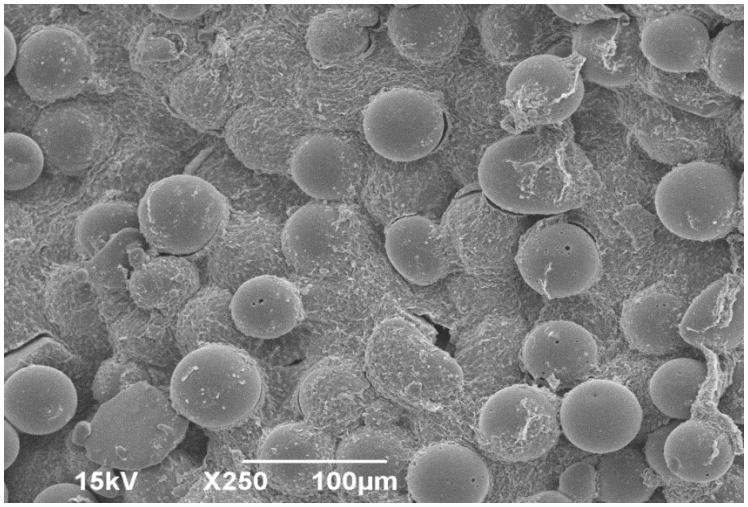

Figure 14. Scanning electron microscope image of 5 g clay and 10 g glass beads membrane.

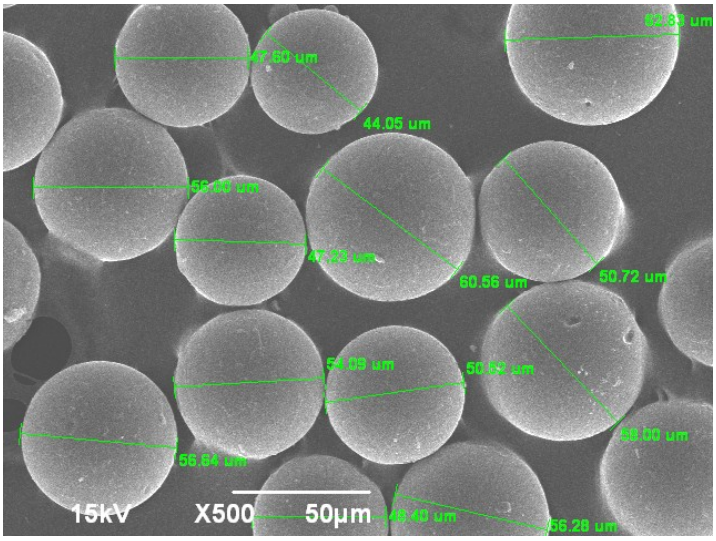

Figure 15. Scanning electron microscope image showing the diameters of the glass beads.

4.2. Solution flux

A comparison of variation in solution flux for different compositions of the clay and glass bead membranes is shown in Figure 16. The solution flux was lowest in the 5 g clay and 10 g glass beads at 2500 psi membrane, followed by the 5 g clay at 2500 psi while the highest flux was observed in the 5 g clay and 10 g glass beads, 500 psi membrane. The impervious glass beads in the clay glass bead mixture reduce the number of pore spaces available for the molecules to pass through; this explains why the 5 g clay and 10 g glass beads membrane had a lower flux than the 5 g clay membrane compacted at the same pressure.

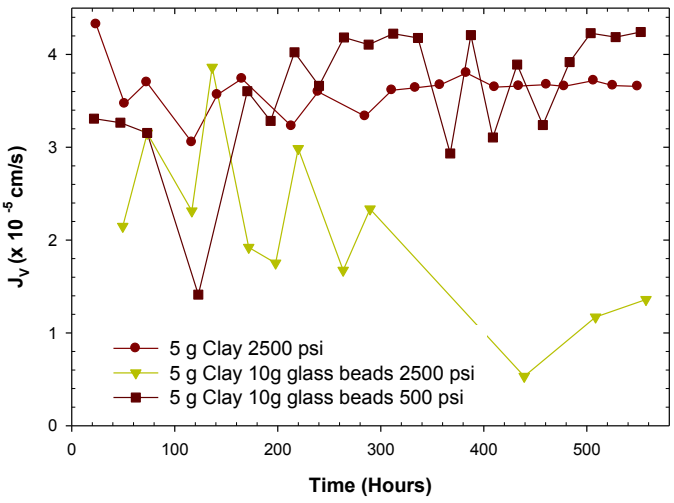

Figure 16. Comparison of solution flux for all the three configurations of clay glass bead membranes.

A lower solution flux was observed in the 5 g clay and 10 g glass beads membrane at 2500 psi compared to 5 g clay and 10 g glass beads compacted at 500 psi. An increase in the compaction pressure reduces the size of the pores in the membrane. Although the 5 g clay and 10 g glass beads at 500 psi membrane has fewer number of pores than 5 g clay at 2500 psi

membrane, due to less compaction, the pore size is generally larger than those in the 5g clay at 2500 psi and therefore offered less resistance to movement of the solution molecules (e.g. Figure 16).

In a membrane, compaction leads to reduction in pore space ratio which is reduced even further with greater compaction (Von Engelhardt and Gaida, 1963). In the design of containment barriers, the lowest obtainable solution flux is not necessarily the optimal flux to achieve when striving for complete containment or remediation of conservative contaminants (Delving and Parker, 1996). The use of containment barriers such as bentonite slurry cutoff walls focus on minimizing the outflow of contaminants; therefore reducing the solution flux may be one of the important parameters in the design of these structures. Other factors may include the reflection coefficient and the composition of the barrier material.

4.3. Reflection coefficient

Rejection coefficient is defined as that portion of the solute that does not permeate through the membrane (Jagur-Grodzinski and Kedem, 1966). The reflection coefficient is expressed as a dimensionless constant range from zero to one (Staverman, 1952). The intrinsic value, which is a good approximation of the reflection coefficient, is given by Equation (7) and is plotted against time for the different configurations of the clay and glass beads membranes (Figure 17). The reduction of reflection coefficient with time has been reported also elsewhere (Demir, 1988; Whitworth, 1994). The reflection coefficient for the three configurations is initially high but gradually reduces. The reflection coefficient varies as a function of both the properties of the clay glass bead membrane, and the properties of the solutions on either side of

the membrane (Whitworth, 2009). In general, an increase in the breakthrough concentration reduces the intrinsic retention of the membrane Equation 7.

In semipermeable membranes, similar to the clay-glass bead mixtures, a high surface charge usually corresponds to a high rejection rate (Oduor, 2004). In the 5 g clay membrane, the rejections rates are higher than those in the mixed 5 g clay and 10 g glass beads at both 500 psi and 2500 psi. There was an overall increase of 30.8%, 23.1%, and 2.2% in the cell concentration of the 5 g clay membrane, 5 g clay and 10 g glass beads at 2500 psi, and 5 g clay and 10 g glass beads at 500 psi membranes respectively. The reflection coefficient is highest at the start of the filtration experiments and slowly wanes off. Solute rejection in clay membranes is affected by membrane surface charge capacity, influent concentration, and the charge of the solute ions (Oduor et al., 2006). An ideal membrane has a value of one which implies that the membrane rejects all the incident solute ions in the solution whereas a value of zero represents a coarse, non-selective membrane where all the solute ions pass through the membrane (Kedem and Katchalsky, 1960).

The surface charge density on the material and the pore space (Fritz and Whitworth, 1994) are major factors that affect the reflection coefficient. The higher the surface charge, the greater the value of the reflection coefficient (Fritz and Whitworth, 1994; Oduor, 2004). In hyperfiltration, where a solution is forced through the clay membrane by a hydraulic gradient, the reflection coefficient is an accepted measure of membrane behavior (Kharaka and Berry, 1974; Fritz, 1983; Oduor, 2004; Odour et al., 2006).

4.4. Membrane filtration coefficient

The membrane filtration coefficient L_P (m^3/N-s) is obtained from Equation (3) for the various solution fluxes J_v, (see appendix Tables A1, A2) and osmotic pressures at various concentrations (Figure 18).

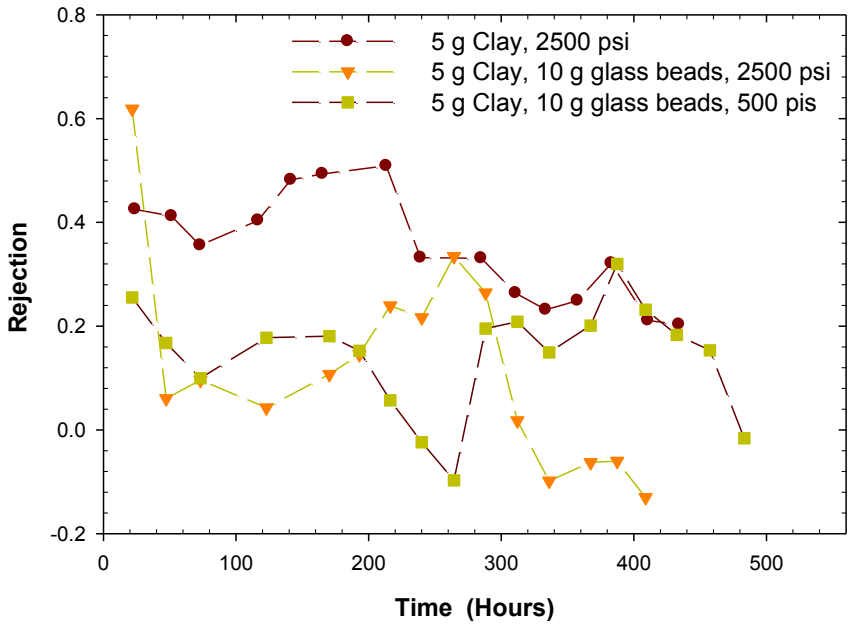

Figure 17. Variation of membrane reflection coefficients of the three configurations of clay-glass bead membranes.

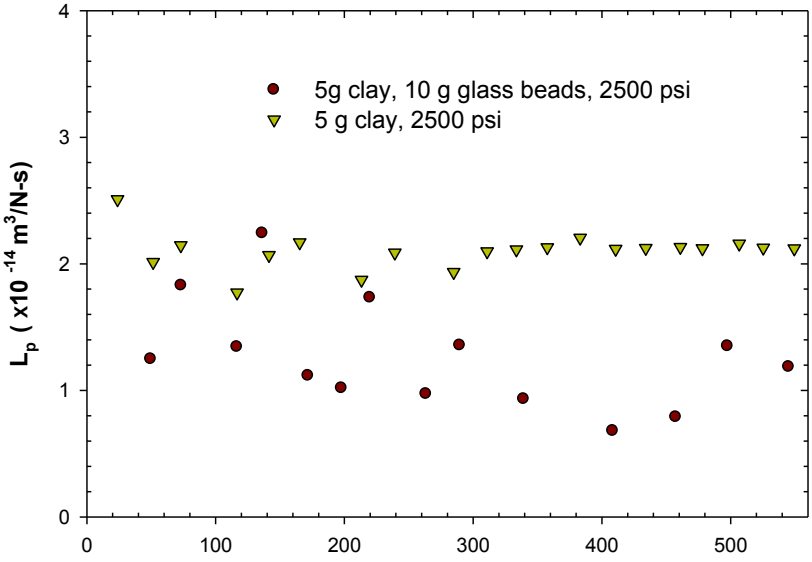

Figure 18.Variation of membrane filtration coefficient L_p of the 5 g clay, 5 g clay and 10 g glass beads at 2500 psi.

There was no significant pressure build up in the 5 g clay and10 g glass beads, 500 psi membrane, to compute L_p. However, the 5 g clay and 10 g glass beads, 2500 psi membrane, experiences a more rapid decline in value to reach a steady state value in comparison to the 5 g clay membrane. The steady state L_p value of 5 g clay and 10 g glass beads, 2500 psi membrane, is much smaller than the steady state L_p value of the 5 g clay membrane compacted at the same pressure.

4.5. Empirical nitrate effluent concentrations

4.5.1. Effects of pressure

To evaluate the effects of pressure on the hyperfiltration of nitrates by the clay-glass beads membranes, the sample compositions of clay-glass beads were subjected to different pressures (i.e. for 500 psi see Figure 19, for 2500 psi see Figure 20 and for 4500 psi see Figure 21). The reduction in nitrate concentration in effluent samples was highest in the membrane of 5 g clay and 10 g glass beads at 4500 psi membrane, followed by 5 g clay and10 g glass beads, 2500 psi membrane system, while that for the 5 g clay and 10 g glass beads, 500 psi membrane system experienced the lowest reduction in the nitrate effluent concentration. Figure 22 shows a comparison of nitrate effluent concentrations of all three pressure settings where nitrate reduction in the systems increases with increasing compaction pressure. Compaction of clay membranes generates a significant overlap of the Gouy layers (see Fig. 2) thereby increasing a likelihood of reduced effluent concentrations especially for permselective membranes. Hence, as the nitrate solution passes through the pores, nitrate anions may have been repelled by the net negative charge on the platelets. An increase in the compaction pressure of the membranes leads also to a decrease in the average pore size. This may also lead to an increase in resistance to flow of advected ions through smaller pores in the membrane.

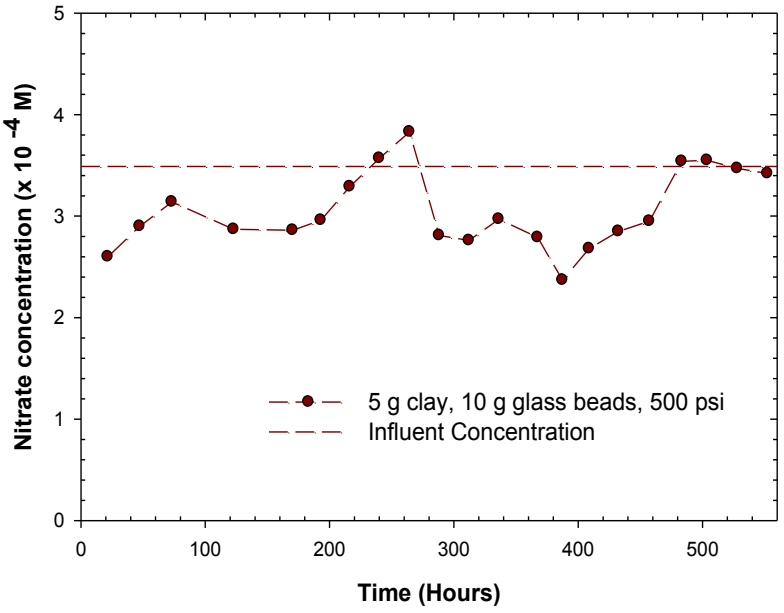

Figure 19. Effluent concentration variation for 5 g clay and 10 g glass beads membrane compacted at 500 psi, where the dashed line shows the nitrate influent concentration.

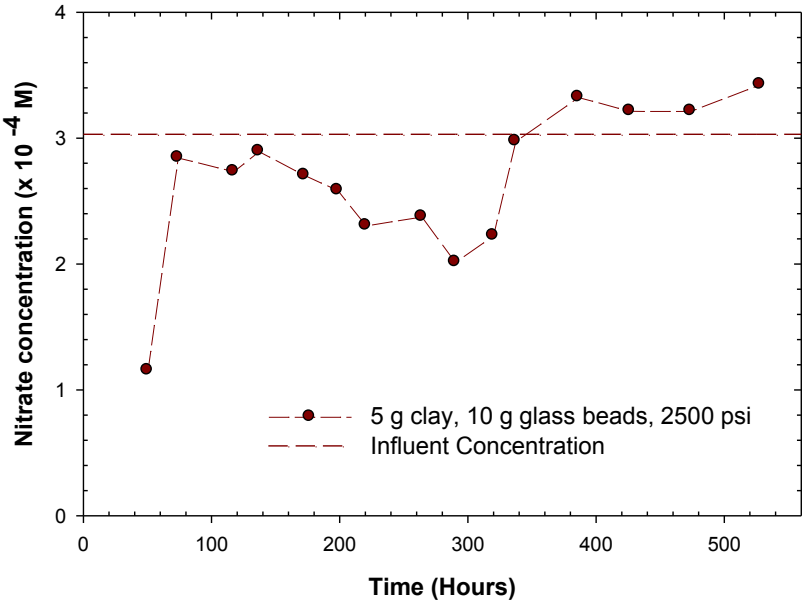

Figure 20. Effluent concentration variation for 5 g clay and10 g glass beads membrane compacted at 2500 psi, where the dashed line shows the nitrate influent concentration.

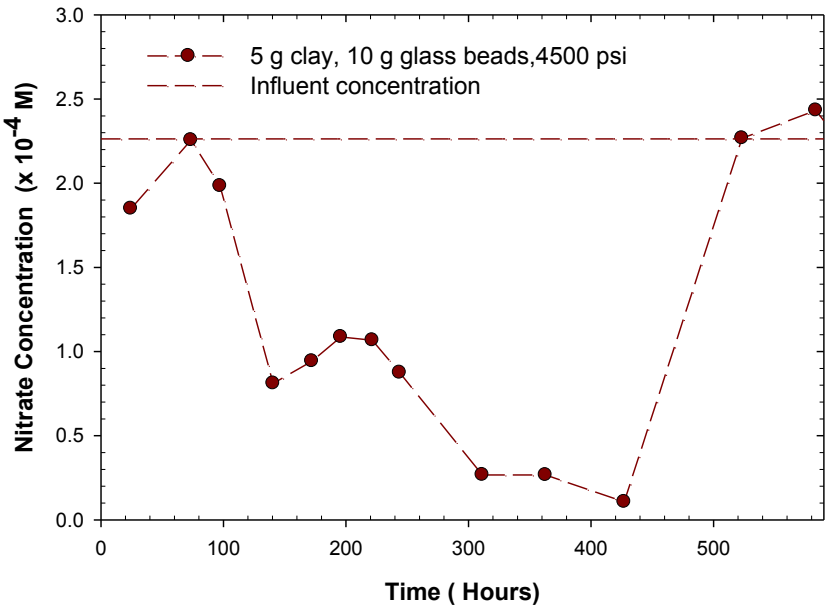

Figure 21. Effluent concentration variation for 5 g clay and10 g glass bead membrane compacted at 4500 psi, where the dashed line shows the nitrate influent concentration.

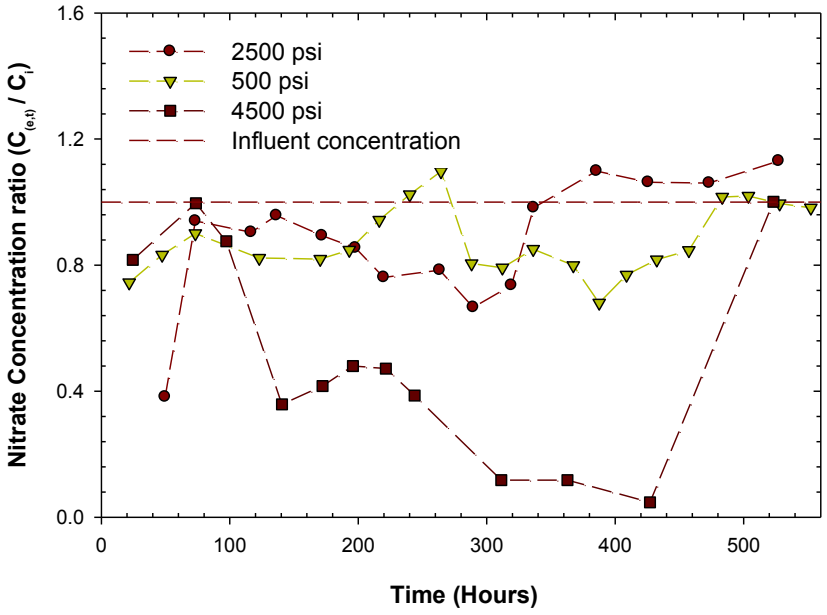

Figure 22. Effluent concentration variation for the 5 g clay and10 g glass bead membrane compacted at the three different pressures, where the dashed line shows the nitrate influent concentration.

4.5.2. Effects of composition

To evaluate the effects of clay composition of the clay–glass beads mixtures; two configurations, one of 5 g clay and the other 5 g clay and 10 g glass beads, were subject to the same pressure, that is, 2500 psi. The reduction in nitrate concentration in effluent samples was higher in the 5 g clay membrane configuration as seen in Figure 23 compared to concentration using the 5 g clay and 10 g glass bead membrane (Figure 24). A comparison of the performance of both membrane configurations in hyperfiltration of nitrates is shown in Figure 25.

In porous media, the proportion of clay in the media affects the osmotic properties and, therefore, the reflection coefficient. Porous media with little or no clay shows no measurable membrane properties and has a reflection coefficient value of zero. The ability of clayey materials to restrict the flow of solutes across a membrane has been reported to improve with an increased amount of bentonite in the soil mixtures amidst little compaction (Garavito Rojas, 2006). This behavior in low permeability clayey materials can be ascribed to the electrical properties of the clay minerals that make up the soil-clay mixture (Garavito Rojas, 2006).

The net negative surface charge on numerous clay minerals surface charge (charge deficiency) is caused by broken bonds and substitution of low valence cations within the lattice (Fritz and Marine, 1983). In clay-rich sediments, double layer thicknesses are significantly large to influence the solution in the pores while solution in non-clayey materials is uninfluenced by the double layers (Garavito Rojas, 2006).

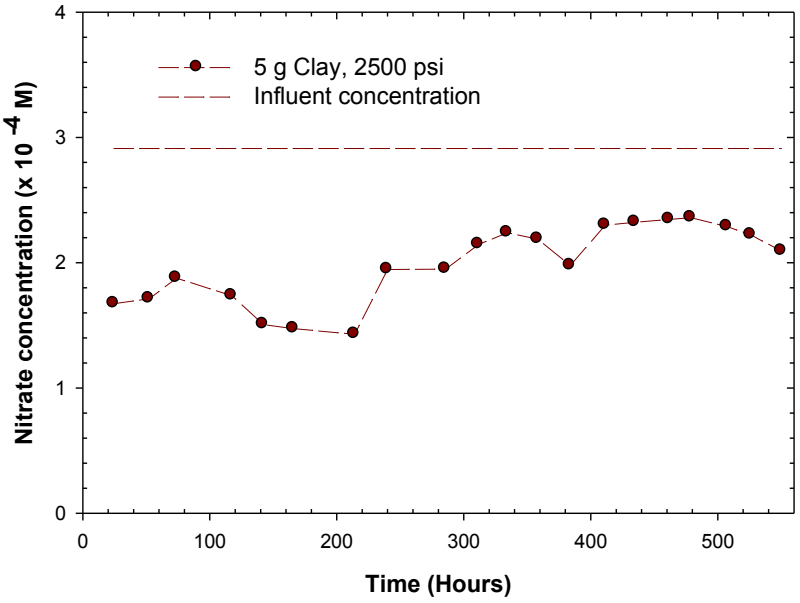

Figure 23. Effluent concentration variation for 5 g clay membrane compacted at 2500 psi, where the dashed line shows the nitrate influent concentration.

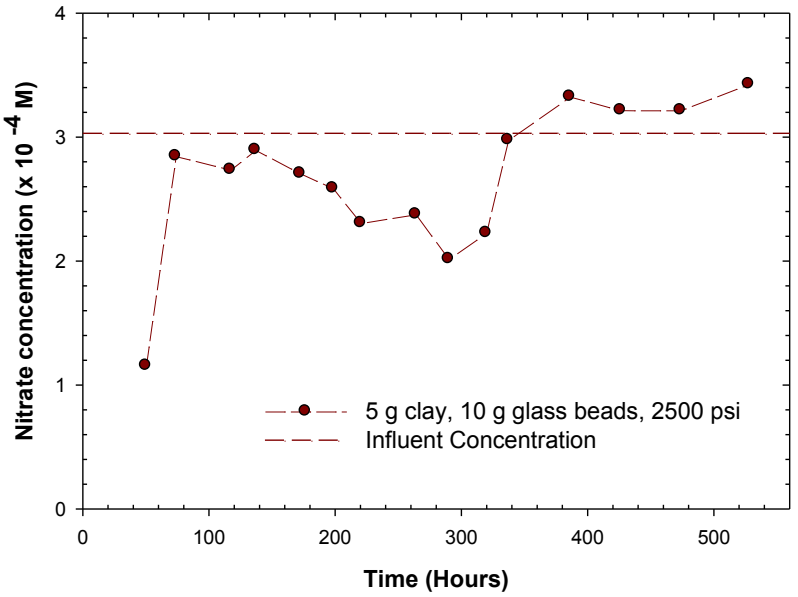

Figure 24. Effluent concentration variation for 5 g clay and 10 g glass beads membrane compacted at 2500 psi, where the dashed line shows the nitrate influent concentration.

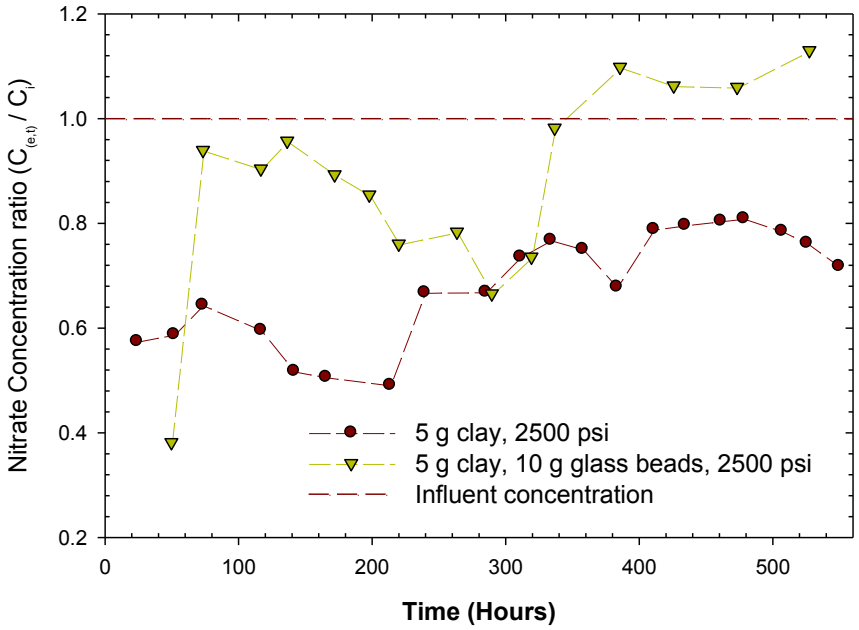

Figure 25. Effluent concentration variation for the two compositions of the membrane, where the dashed line shows the nitrate influent concentration.

4.6. Modeling

Effluent concentrations were modeled using Equations (10) and (11), see (appendix Tables A1, A2, A3) for the three configurations of the membranes (i.e. 5 g clay at 2500 psi, 5 g clay and10 g glass beads at 2500 psi and, 5 g clay and 10 g glass beads at 500 psi) Figure 26.

The model was tested using experimental data for the three membrane configurations (Figures 27, 28, and 29). The solution flux value used was similar to values obtained in the experiment (Table A1). An empirically determined average membrane thickness of 4 mm and area of 38.4cm^2 were used in the model. The solute diffusion coefficient, *D*, for free nitrate ions used was 1.846 1.31×10^{-9} m^2 s^{-1} (for example Weast and Astle, 1986).

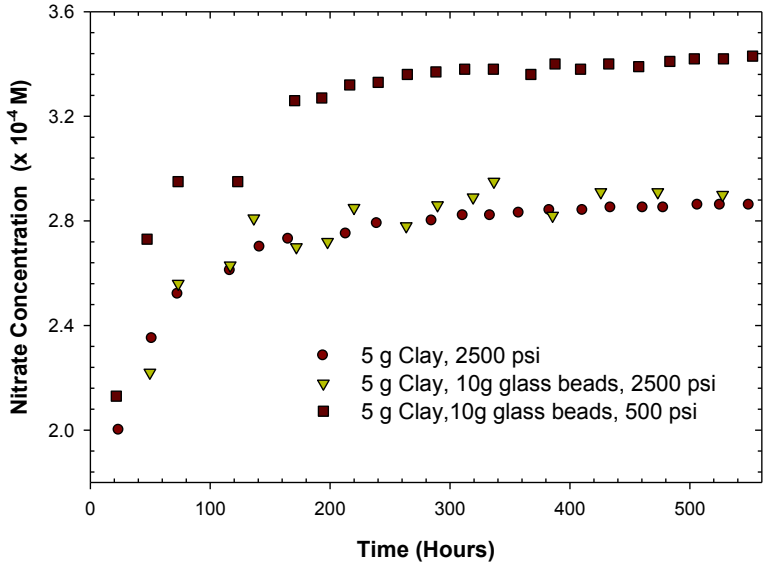

Figure 26. Modeled effluent concentrations for all membranes systems.

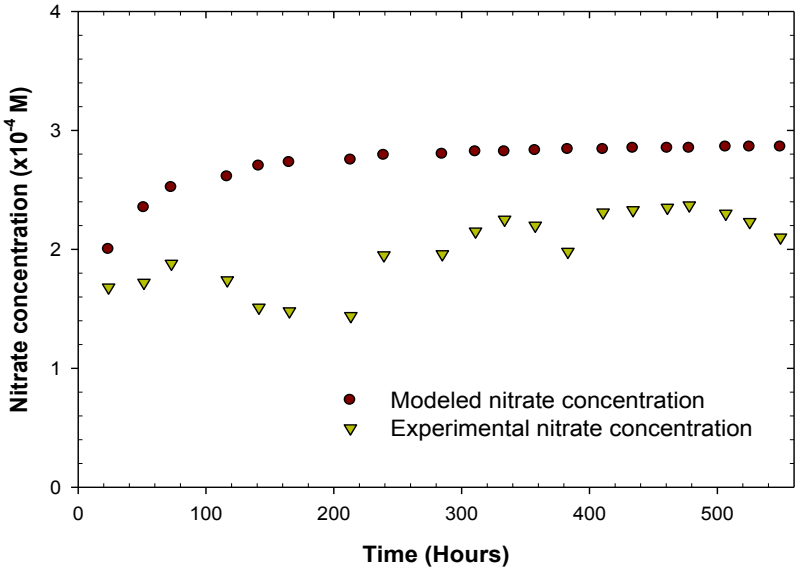

Figure 27. A comparison between the modeled effluent concentration and the experimental concentration for the 5 g clay membrane at 2500 psi.

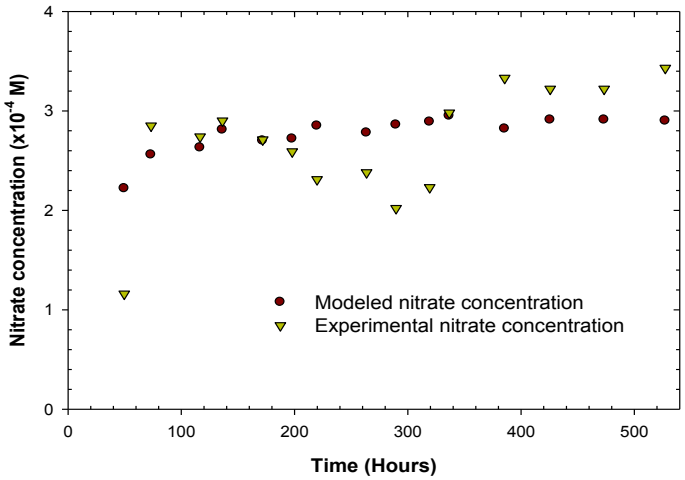

Figure 28. A comparison between the modeled effluent concentration and the experimental concentration for the 5 g clay and 10 g glass beads membrane at 2500 psi.

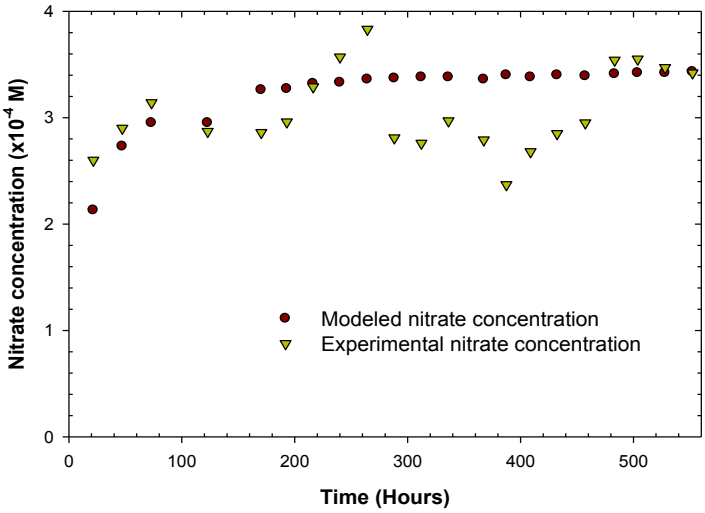

Figure 29. A comparison between the modeled effluent concentration and the experimental concentration for the 5 g clay and 10 g glass beads membrane at 500 psi.

4.7. Error analysis

The experimental accuracies may have been affected by several factors briefly discussed below. At the final time step when the experiment was stopped, the cell solution was collected and the nitrate concentration was analyzed. A mass balance was computed for the three

membrane configurations (see Tables 2, 3, 4). The mass balance for the nitrate ions was computed by summing the nitrate ions in the reservoir solution and the nitrates ions in both the collected samples and hyperfiltration cell residue. The results are presented as a percentage difference between input and output of nitrate ions from the system.

Table 2. Summary of mass balance calculations for 5 g clay at 2500 psi.

Input	**Influent Nitrates**	**C_i x Total volume**	**0.979**	**(x 10^{-3} mol)**
Output	Collected (samples) Nitrates		0.552	(x 10^{-3}mol)
	Cell Nitrate	Cell Volume x C_{cell}	0.210	(x 10^{-3} mol)
Difference	Difference	input - output	0.216	(x 10^{-3} mol)
	Percentage Difference		22.10	

Table 3. Summary of mass balance calculations for 5 g clay and 10 g glass beads at 2500 psi.

Input	**Influent Nitrates**	**C_i x Total volume**	**0.660**	**(x 10^{-3} mol)**
Output	Collected (samples) Nitrates		0.434	(x 10^{-3} mol)
	Cell Nitrate	Cell Volume x C_{cell}	0.205	(x 10^{-3} mol)
Difference	Difference	input - output	0.021	(x 10^{-3} mol)
	Percentage Difference		3.23	(%)

Table 4. Summary of mass balance calculations for 5 g clay and 10 g glass beads at 500 psi.

Input	**Influent Nitrates**	**C_i x Total volume**	**1.097**	**(x 10^{-3} mol)**
Output	Collected (samples) Nitrates		0.902	(x10^{-3} mol)
	Cell Nitrate	Cell Volume x C_{cell}	0.181	(x10^{-3} mol)
Difference	Difference	input - output	0.014	(x10^{-3} mol)
	Percentage Difference		1.28	(%)

The percentage difference in mass balance for 5 g clay and 10 g glass bead membrane at 500 psi and 2500 psi may be acceptable within limits of error. However, percentage difference

(i.e. 22%) for the 5 g clay membrane at 2500 psi was high. Larger percentage differences in mass balance of ions through compacted clay have been previously reported (for example Shackelford et al., 1989). Among the possible sinks for the nitrate ions in compacted clay membranes is the formation of complex species with cations in the bentonite.

In the experimental analysis, potential sources of error include dilution of the nitrate solution by the de-ionized water in the membrane. Experimental errors that probably affected the mass balance calculations are the variation in the operating pressure in the cell. Variation in pressure affects the compaction of the membrane during the experiment. When nitrate solution was passed through the membrane and a portion of the solute was adsorbed in the clay membrane or clay-glass bead membrane, this portion was not accounted for in the mass balance. The precision of chemical analysis could have introduced some errors associated with instrumentation to the mass balance errors. Efforts to minimize errors included taking an average concentration of three replicates.

There are errors in assuming that the value of $C_{(0,t)}$ remained constant during the sample collection which overstates the value of $C_{(0,t)}$ (Oduor et al., 2009) and implicitly overstates the value of the modeled break-through concentration $C_{(e,t)}$. Temperature variation may also affect the flux of the solutes and solutions through the membranes, and therefore results of break-through effluent concentrations need to be thermally-invariant since the basic governing equations were developed for isothermal conditions (Fritz,1983; Oduor 2004). While modeling the break-through concentrations, variation in the temperature of the feed to the membranes was considered to be negligible yet an experimental temperature variation of 3 ^{o}C was observed.

5. CONCLUSIONS

A brief introduction to hyperfiltration and the factors that influence the movement of inorganic contaminants such as nitrate ions across compacted membrane barriers (e.g. bentonite cutoff walls and geosynthetic clay liners) are presented in this study. The equations defining solution flux, intrinsic retention and the membrane filtration coefficient in semipermeable membranes used in waste containment structures are also briefly discussed. An analysis of results using various volumetric compositions of clay and glass beads are also presented and discussed. The compaction of the membranes represented by different pressures was shown to have the most deterministic influence on the amount of solute ions sieved off by the membrane; this is as a result in both the reduction in solution flux and also manifested as an increase in the rejection of solute ions by the membrane. The composition of the membranes, represented by the ratio of glass beads to clay, was critical in altering breakthrough concentration. The high clay composition membrane exhibited better rejection efficiencies. The solution flux was higher through the lower clay content membrane compacted at the same pressure as the high clay content membrane. However, a reduction in both compaction pressure and bentonite content in the clay glass beads mixture led to a drastic reduction in nitrate removal capacity of the clay glass beads membrane. There was an overall increase of 30.8%, 23.1%, and 2.2% in the cell concentration of the 5 g clay membrane, 5 g clay and 10 g glass beads at 2500 psi, and 5 g clay and 10 g glass beads at 500 psi membranes, respectively. The results show that hyperfiltration of nitrate ions is not simply a function of the compaction pressure but also varies with composition of bentonite in the mixed membrane which increases the surface charge of the membrane. High

bentonite content membranes compacted at an optimal pressure offered the best potential to nitrate contaminant remediation.

The effluent nitrate concentrations, $C_{(e,t),}$ were modeled and compared fairly well with experimentally derived nitrate concentrations for various configurations of the clay-glass beads membrane. However, the model overestimates the breakthrough concentrations for the 5g clay membrane at 2500 psi. The difference in the experimental and modeled effluent concentrations stems from the approximation of concentrations adjacent to high pressure side $C_{(0,t)}$ and the value chosen for diffusion coefficient D, which is diffusion of the free nitrate ions yet in porous media, value may be lower. Future research should look at accurately quantifying the diffusion in compacted clay membranes.

6. REFERENCES

Abichou, T., Benson, C.H., Edil, T.B., 2002. Micro-structure and hydraulic conductivity of simulated sand–bentonite mixtures. *Clay and Clay Minerals* 50: 537–545.

Anderson, D. M., Kaoru, Y., White, A.W. (2000). Estimated annual economic impacts from harmful algal blooms (HABs) in United States. *Woods Hole Oceanographic Institute Technical Report, WHOI-2000-11.*

Bardot, C., Gaubert, E., Yaroshuk, A. (1995). Unusual mutual influence of electrolytes during pressure-driven transport of their mixtures across charged porous membranes. *Journal of Membrane Science*, 103:11-18.

Beeson S. and Cook, M.C. (2004). Nitrate in groundwater: a water company perspective. *Quarterly Journal of Engineering Geology and Hydrogeology*, 37 (4): 261-270.

Bergaya, F. and Lagaly, G. (2006). (Eds.). General Introduction: Clays, Clay Minerals, and Clay Science. Handbook of Clay Science: *Developments in Clay Science*, 1: 1-18.

Berry, F.A.F. (1967). Role of membrane hyperfiltration on origin of thermal brines, Imperial valley, California: *The American Association of Petroleum Geologists Bulletin* 51 (3): 454-455.

Birkeland, P. (1999). *Soils and Geomorphology*, third edition. 430.

Burden, R. J. (1982). Nitrate contamination in New Zealand aquifers: a review. *New Zealand Journal of science*. 25 (3): 205-220.

Cheng, F., Muftikian, R., Fernando, Q., Korten, N. (1997). Reduction of nitrate to ammonia by zero valent iron. *Chemosphere* 35: 2689-2695.

Cheshire, M.V., Sparking, G.P., Mundie, C.M. (1983). Effect of periodate treatment of soil on carbohydrate constituents and soil aggregation. *Journal* of *Soil Science* 34: 10-112.

Cheung, V.V., Galloway, T.S., Depledge, M.H. (2011). Chemical disruption of biologiphenomenanoma. *Chemical Ecology*. Accessed online April 03 2012. http://www.eolss.net/Eolss-sampleAllchapter.aspx

Coplen, T.B., Hanshaw, B.B. (1973) Ultrafiltration by a compacted membrane—I. Oxygen and hydrogen isotope fractionation. *Geochimica et Cosmochimica Acta* 37: 2205-2310.

Davis, R.H. (1992). *Theory of cross flow microfiltration*. In: W.S.W. Ho, K.K. Sirkar (Eds.), Membrane Handbook, Van Nostrand Reinhold. 480-505.

De la Fuente García-Soto, M.M., Muñoz Camacho, E. (2005). Boron removal industrial wastewaters by ion exchange: an analytical control parameter. *Desalination* 181: 207-216.

Devlin, J.F., Parker, B.L. (1996). Optimum hydraulic conductivity to limit contaminant flux through cutoff walls. *Ground water* 34: 719-726.

Demir, I., (1988). Studies of smectite membrane behavior: electrokinetic, osmotic, and isotopic fractionation processes at elevated pressures. *Geochimica et Cosmochimica Acta* 52: 727-737.

Derrington, D., Hart, M., Whitworth, T.M. (2006). Low head sodium phosphate and nitrate hyperfiltration through thin kaolinite and smectite layers -Application to engineered systems. *Applied Clay Science* 33: 52-58.

Dijk, H.W.J., de Groot, V.W.T. (1987). Eutrophication of a coastal dune area by artificial infiltration. *Water Research* 21(1): 11-18.

Dorworth, L.E. (2003). Understanding Why Some Organic Contaminants Pose a Health Risk. Department of Biological Sciences Purdue University Calumet Hammond, IN accessed on April 04- 2012. http://www.iisgcp.org/catalog/downlds_09/wic_orgcont.pdf

Elimelech, M., Zhu, X., Childress, A.E., Hong, S. (1997). Role of membrane surface morphology in colloidal fouling of cellulose acetate and composite aromatic polyamide reverse osmosis membranes. *Journal of Membrane Science* 127: 101-109.

Fan, A.M., Steinberg, V.E. (1996). Health Implications of Nitrate and Nitrite in Drinking Water: An Update on Methemoglobinemia Occurrence and Reproductive and Developmental Toxicity. *Regulatory Toxicology and Pharmacology*. 23(1):35-43,

Fann C.B., Kaneene, J.B., Miller, R.A., Gardner, I., Johnson, R., Ross, F. (1994). The use of epidemiological concepts and techniques to discern factors associated with the nitrate concentration of well water on swine farms in the USA. *Science of the Total Environment* 153(1-2): 85-96.

Favre F., Tessier, D., Abdelmoula, M., Génin, J.M., Gates, W.P., Boivin, P. (2002). Iron reduction and changes in cation exchange capacity in intermittently water logged soil. *European Journal of Soil Science* 53: 175-18.

Favre, F., Bagdad, C., Gaveled, S., Stucki, J.W. (2006). Changes in the CEC of a soil smectite–kaolinite clay fraction as induced by structural iron reduction and iron coatings dissolution. *Applied Clay Science* 34: 95-104.

Ferreira, J.G., Brickerb, S.B., Simasa, T.C. (2007). Application and sensitivity testing of a eutrophication assessment method on coastal systems in the United States and European Union. *Journal of Environmental Management* 82: 433-445.

Filgueira, R.R., Fournier, L.L., Cerisola, C.I., Gelati, P., García, M.G. (2006). Particle-size distribution in soils: A critical study of the fractal model validation. *Geoderma* 134: 327-334.

Fritz, S.J., Whitworth, T.M. (1994). Hyperfiltration-induced fractionation of lithium isotopes-ramifications relating to representativeness of aquifer sampling. *Water Resources Research* 30: 225-235.

Fritz, S. J., Eady, C.D. (1985). Hyperfiltration-induced precipitation of calcite. *Geochimica et Cosmochimica Acta* 49: 761-768.

Fritz, S.J., Marine, I.W. (1983). Experimental support for a predictive osmotic model of clay membranes. *Geochimica et Cosmochimica Acta*, 47: 1515-1522.

Gatseva, P.D., Mariana, D.A. (2008). High-nitrate levels in drinking water may be a risk factor for thyroid dysfunction in children and pregnant women living in rural Bulgarian areas. *International Journal of Hygiene and Environmental Health* 211: 555-559.

Goldsmith, H., Lolachi, H. (1970). Test Cell for Measuring the Concentration Polarization Boundary Layer in a Reverse Osmosis System, United States Department of the Interior, Washington, DC 20402, Research and Development Progress Report.

Graf, D.L. (1982). Chemical osmosis, reverse osmosis, and the origin of subsurface brines. *Geochimica et Cosmochimica Acta*, 46: 1431-1448.

Garavito Rojas, A.M.F. (2006). Chemical osmosis in clayey sediment. PhD thesis,Vrije Universiteit, Amsterdam, The Netherlands.

Griggs, E.M., Kump, L.R., Böhlke, J.K. (2003). The fate of wastewater-derived nitrate in the subsurface of the Florida Keys: Key Colony Beach, Florida: *Estuarine, Coastal and Shelf Science* 58(3): 517-539.

Guichet, X., Fleuryb, M., Kohlerc, E. (2008). Effect of clay aggregation on water diffusivity using low field NMR. *Journal of Colloid and Interface Science* 327: 84-93.

Hart, M., Whitworth, T.M., Atekwana, E. (2008). Hyperfiltration of sodium chloride through kaolinite membranes under relatively low-heads - Implications for groundwater assessment: *Applied Geochemistry* 23: 1691-1702.

Hashim, M.A., Mukhopadhyay, S., Sahu, J. N., Sengupta, B. (2011). Remediation technologies for heavy metal contaminated groundwater. *Journal of Environmental Management* 92 (10): 2355-2388.

Heister, K. (2005). Coupled transport in clayey materials with emphasis on induced electrokinetic phenomena. PhD thesis, KatjaUniversiteit Utrecht, The Netherlands.

Huang, J., Guo, Q., Ohia, H., Fang, J. (1998). The characteristics of crosslinked PAA composite membrane for separation of aqueous organic solutions by reverse osmosis. *Journal of Membrane Science* 144: 1-11.

Hwang, Y., Kim, D., Shin, H. (2011). Mechanism study of nitrate reduction by nano zero valent iron. *Journal of Hazardous Materials* 185(2-3): 1513-1521.

Ishiguro, M., Matsuura, T., Detellier,C. (1995). Reverse osmosis separation for a montmorillonite membrane. Journal of Membrane Science, 107: 87-92.

Jagur-Grodzinski, J., Kedem, O. (1966). Transport coefficients and salt rejection in unchanged hyperfiltration membranes. *Desalination* 1:327-341

Jiang, W., Childs, R.F., Mika, A.M., Dickson J.M. (2003). Pore-filled Membranes Capable of Selective Negative Rejections. *Nature and Science* 1: 21-25.

Kabay, N., Sarp, S., Yuksel, M., Kitis, M., Koseiglu, H., Arar, O., Bryjak, M., Semiat, R. (2008). Removal of boron from SWRO permeate by boron selective ion exchange resins containing N-methyl glucamine groups. *Desalination* 223: 49-56.

Kang, J.B. Shackelford, C.D. (2009). Clay membrane testing using a flexible-wall cell under closed-system boundary conditions: *Applied Clay Science* 44: 43-58.

Kasper, J.W. (2007). Simulated ground-water flow at the Fairmount Site, Sussex County, Delaware (USA), with implications for nitrate transport. PhD. thesis, University of Delaware, 145.

Keijzer, T.J.S. (2000). Chemical osmosis in natural clayey materials. PhD. thesis, Universiteit Utrecht, Netherlands, 166.

Krešić, N., Stevanović, Z. (2010). *Groundwater hydrology of springs: engineering, theory, management, and sustainability*. 251.

Kharaka, Y., Berry, F.A. (1974). Simultaneous flow of water and solutes through geological membranes I; Experimental investigation. *Geochimica et Cosmochimica Acta* 37: 2577-2603.

Kim, J., Benjamin, M.M. (2004). Modeling a novel ion exchange process for arsenic and nitrate removal. *Water Research* 38: 2053-2062.

Kooi, H., Garavito, A.M., Bader, S. (2003). Numerical modeling of chemical osmosis and ultrafiltration across clay formations: *Journal of Geochemical Exploration* 78-79: 333-336.

Lange, K., Rowe, R.K., Jamieson, H. (2010). The potential role of geosynthetic clay liners in mine water treatment systems: *Geotextiles and Geomembranes* 28: 199-205.

Liangxiong, L., Whitworth, T.M., Lee, R. (2003). Separation of inorganic solutes from oil-field produced water using a compacted bentonite membrane. *Journal of Membrane Science* 217(1-2): 215-225.

Martin, R.T., Bailey, S.W., Eberl, D.D., Fanning, D.S., Guggenheim, S., Kodama, H., Pevear, D. R., Srodon, J., Wicks, F.J. (1991). Report of the clay minerals society nomenclature committee: revised classification of clay materials. *Clays Clay Miner* 39(3): 333-335.

Merten, U. (Ed.) (1966). *Desalination by Reverse Osmosis*. MIT Press, Cambridge.

Metcalf, A., Eddy, V., 2003. Wastewater Engineering, Treatment and Reuse, 4th edition. McGraw Hill, New York.

Mulder, M.H.V. (1995). Polarization phenomena and membrane fouling. *Membrane Separations Technology, Principles and Applications (*eds. R. D. Noble and S. A. Stern). 50-83.

Mulder, M. (1996*). Basic Principles of Membrane Technology*. Kluwer Academic Publishers, Boston.

Munster, J. E. (2008). Nonpoint sources of nitrate and perchlorate in urban land use to groundwater, Suffolk County, NY. PhD thesis Stony Brook University.

Nijboer, R.C., Verdonschot Piet, F.M. (2004). Variable selection for modeling effects of eutrophication on stream and river ecosystems. *Ecological Modeling* 177: 17-39.

Nolan, B.T. and Stoner, J.D. (2000). Nutrients in ground waters of the conterminous United States, 1992 -1995. *Environmental Science and Technology* 34 (7): 1156-1165.

Oduor, P.G., Gibbs, P., Santos, X., Podoll, A., Dunham, J. (2009). Organo-macromolecular transport relationships for argillaceous membranes at ultra-high hydraulic gradients: *Desalination* 239: 175-190.

Oduor, P.G., Casey, F.X., Podoll, A. (2006). Modeling of concentration polarization layer evolution and breakthrough concentrations in dead-end hyperfiltration: *Journal of Membrane Science* 285: 376-384.

Oduor, P.G. and Whitworth, T.M. (2005). Mechanistic interpretation of ionic azo dye flux decline through compacted Na-montmorillonite membrane: *Journal of Membrane Science* 265: 85-93.

Oduor, P.G. and Whitworth, T.M. (2004). Transient modeling of hyperfiltration effects, *Mathematical Geology* 36: 743-758.

Okafor, P.N. and Ogbonna, U.I. (2003). Nitrate and nitrite contamination of water sources and fruit juices marketed in South-Eastern Nigeria. *African Journal of Biotechnology* 4 (10): 1105-1108.

Peñate, B. and García-Rodríguez, L. (2012). Current trends and future prospects in the design of seawater reverse osmosis desalination technology. *Desalination* 284: 1-8.

Probstein, R.F., Chan, K. K., Cohen, R., Rubenstein, I. (1981). Model and preliminary experiments on membrane fouling in reverse osmosis. *Synthetic Membranes Desalination ACS Symposium*, I: 131-145.

Shen, S., Stucki, J.W., Boast, C. W. (1992). Effects of structural iron reduction on the hydraulic conductivity of Na-Smectite. *Clays and Clay Minerals*: 40 (4), 381-386.

Schäfer, R.B. (2012). Biodiversity, ecosystem functions and services in environmental risk assessment*:* Introduction to the special issue*. Science of the Total Environment* 415: 1-2.

Redondo, J.A. and Witte, J.P.M.B. (2003). Boron removal from sea water using FILMTEC™ high rejection SWRO membranes. *Desalination* 156: 229-238.

Rhoades, J.D. (1982). Cation exchange capacity, In: Page, A.L., Miller, R.H., Keeney, D.R.(Eds.), *Methods of soil analysis, Part 2: Chemical and microbiological properties*, 2nd ed., Series Agronomy, 9. ASA - SSSA, Madison, 149-157.

Rivett, M.O., Smith, J.W.N., Buss, S.R., Morgan, P. (2007). Nitrate occurrence and attenuation in the major aquifers of England and Wales. *Quarterly Journal of Engineering and Hydrogeology* 40(4): 335-352.

Rodríguez-Maroto J.M., García-Herruzo, F., García-Rubio, A., Gómez-Lahoz, C., Vereda-Alonso, C. (2009). Kinetics of the chemical reduction of nitrate by zero-valent Iron. *Chemosphere* 74: 804-809.

Rodríguez P.M., Ferrandiz, R.A., Arias, M.F.C., Rico, D.P. (2001). Influence of pH in the elimination of boron by means of reverse osmosis. *Desalination* 140: 145-152.

Saffaj, N., Loukili, H., Alami-Younssi, A., Albizane, A., Bouhria, M., Persin, M., Larbot A. (2004). Filtration of solution containing heavy metals and dyes by means of ultrafiltration membranes deposited on support made of Morrocan clay. *Desalination* 168: 301-306.

Saindon, R. and Whitworth, T.M. (2006). Reverse osmosis properties of bentonite /glass bead mixtures at low compaction pressures: *Applied Clay Science* 31: 90-95.

Schmidt, D.R., Ghosh, P., Katti, K.S., (2005). Modeling Response of Pyrophyllite Clay Interlayer to Applied Stress Using Steered Molecular Dynamics. *Clays and Clay Minerals* 52(2):171-178.

Shaalan, H.F. (2002). Development of fouling control strategies pertinent to nanofiltration membranes. *Desalination* 153:125-131.

Shrimali, M., Singh, K.P. (2000). New methods of nitrate removal from water. *Environmental Pollution* 112: 351-359.

Shirazi, S., Lin, C., Chen, D. (2010). Inorganic fouling of pressure-driven membrane processes-A critical review. *Desalination* 250: 236-248.

Shirazi, S.H., Lin, C.J., Doshi, S., Agarwal, S., Rao, P. (2006). Comparison of fouling mechanism by $CaSO_4$ and $CaHPO_4$ on nanofiltration membranes. *Separation Science and Technology* 41: 2861-2882.

Spalding, R.F., Exner, M.E., Martin, G.E., Snow, D.D. (1993). Effects of sludge disposal on groundwater nitrate concentrations. *Journal of Hydrology* 142 (1-4): 213-228.

Srivastava, R.C. and Jain, A.K. (1975). Non-equilibrium thermodynamics of electro-osmosis of water through composite clay membranes. The electro-kinetic energy conversion: *Journal of Hydrology* 25: 307-324.

Strathmann, H. (1968). Concentration polarization in reverse osmosis desalination of water: Research and Development Progress Report No. 336, U. S. Dept. of the Interior, Washington, D.C., 96.

Stucki, J.W. (1997). Redox processes in smectites: soil environmental significance. *Advances in GeoEcology* 30: 395-406.

Staverman, A.J. (1952) Non-equilibrium thermodynamics of membrane processes. *Transactions of the Faraday Society* 48: 176-185.

Shackelford, C.D., Daniel, D.E., Liljestrand, H.M. (1989). Diffusion of inorganic chemical species in compacted clay soil. *Journal of Contaminant Hydrology* 4: 241 273.

Tsuru, T., Nakao, S., Kimura, S. (1991). Calculation of ion rejection by extended Nernst-Planck equation with charged reverse osmosis membranes for single and mixed electrolyte solutions. *Journal of Chemical Engineering of Japan* 24(4): 511-517.

Urairi, M., Tsuru, T., Nakaob, S., Kimura, S. (1992). Bipolar reverse osmosis membrane for separating mono-and divalent ions. *Journal of Membrane Science* 70(2-3): 153-16.

Von Engelhardt,W., Gaida, K.H. (1963). Concentration changes of pore solutions during compaction of clay sediments. *Journal of Sedimentary Research* 33: 919-930.

Weisbrodt, J., Maunthey, M., Ditgens, B., Laufenberg, G., Kunz, B. (2001). Separation of aqueous organic multi-component solutions by reverse osmosis—development of a mass transfer model. *Desalination* 133: 65-74.

Weast, R.C., Astle, M.J. (eds.) (1981). *Handbook of Chemistry and Physics*, 62 nd edition 1981-1982. CRC press Inc. Boca Raton, Florida.

Westerhoff, P., James, J. (2003).Nitrate removal in zero-valent iron packed columns. *Water Research* 37: 1818-1830.

Whitworth, T.M., Ghazifard, A. (2009). Membrane effects in clay-lined inward gradient landfills. *Applied Clay Science* 43(2): 248-252.

Wiesner, M.R., Theis, T.L. (1996). Environmental engineering education: Application area and discipline. *Journal of Environmental Engineering-Asce* 122 (2): 89-90.

Wijmans, J.G., Nakao, S., Van Den Berg, J.W.A., Troelstra, F.R., Smolder, C.A. (1985). Hydrodynamic resistance of concentration polarization boundary layers in Ultrafiltration: *Journal of Membrane Science* 22: 117-135.

Yoo, D.J., Oh, M., Kim, Y.S., Park, J. (2009). Influences of solution and mixed soil on estimating bentonite content in slurry using electrical conductivity. *Applied Clay Science* 43: 408-414.

Zhang, W.L., Tian, Z.X., Zhang, N., Li, X.Q. (1996). Nitrate pollution of Northern China. *Agriculture, Ecosystems and Environment* 59(3): 233-231.

Zhang D., Zhou, C., Lin, C., Tong, D., Yu, W. (2010). Synthesis of clay minerals. *Applied Clay Science* 50: 1-11.

7. APPENDIX

Table A1. Summary of selected calculated parameters for the 5 g clay membrane at 2500 psi.

Mass (g)	Time (Hours)	[a] Jv (cm/s)	[b] L_p (m^3/N-s)	[c] $C_{(0,t)}$ (M)	[d] $C_{(e,t)}$(M)	[e] σ	$C_{(experiment)}$	C_{et}/C_i
	0						0.000292	1.000000
141.995	23.75	$4.32 X^{-05}$	$2.09 x10^{-13}$	0.000584	0.000200	0.49	0.000168	0.574963
133.050	51.48	$3.47 X^{-05}$	$1.26 x 10^{-13}$	0.000585	0.000235	0.45	0.000172	0.588169
109.720	72.93	$3.70 X^{-05}$	$1.07 x 10^{-13}$	0.000585	0.000252	0.39	0.000188	0.644545
184.510	116.62	$3.05 X^{-05}$	$6.82 x 10^{-14}$	0.000585	0.000261	0.39	0.000174	0.596373
122.098	141.38	$3.57 X^{-05}$	$6.08 x 10^{-14}$	0.000585	0.000270	0.34	0.000151	0.518035
123.520	165.28	$3.74 X^{-05}$	$6.02 x 10^{-14}$	0.000585	0.000273	0.33	0.000148	0.506631
214.525	213.35	$3.23 X^{-05}$	$4.26 x 10^{-14}$	0.000585	0.000275	0.35	0.000144	0.491235
128.620	239.20	$3.60 X^{-05}$	$4.35 x 10^{-14}$	0.000585	0.000279	0.31	0.000195	0.668144
210.445	284.85	$3.33 X^{-05}$	$3.12 x 10^{-14}$	0.000585	0.000280	0.33	0.000196	0.669229
129.792	310.82	$3.62 X^{-05}$	$3.18 x 10^{-14}$	0.000585	0.000282	0.29	0.000215	0.736292
114.785	333.62	$3.64 X^{-05}$	$2.93 x10^{-14}$	0.000585	0.000282	0.29	0.000225	0.768481
121.570	357.57	$3.67 X^{-05}$	$2.66 x 10^{-14}$	0.000585	0.000283	0.28	0.000220	0.750952
134.110	383.08	$3.80 X^{-05}$	$2.69 x 10^{-14}$	0.000585	0.000284	0.28	0.000198	0.679088
138.975	410.63	$3.65 X^{-05}$	$2.46 x 10^{-14}$	0.000585	0.000284	0.28	0.000231	0.789082
118.340	434.02	$3.66 X^{-05}$	$2.36 x 10^{-14}$	0.000585	0.000285	0.28	0.000233	0.797138
136.550	460.88	$3.68 X^{-05}$	$2.32 x 10^{-14}$	0.000585	0.000285	0.28	0.000235	0.804918
87.050	478.10	$3.66 X^{-05}$	$2.12 x 10^{-14}$	0.000585	0.000285	0.27	0.000237	0.809664
146.740	506.63	$3.72 X^{-05}$	$2.16 x 10^{-14}$	0.000585	0.000286	0.27	0.000230	0.785495
94.765	525.33	$3.67 X^{-05}$	$2.13 x10^{-14}$	0.000585	0.000286	0.27	0.000223	0.762687
121.495	549.37	$3.66 X^{-05}$	$2.16 x 10^{-14}$	0.000585	0.000286	0.27	0.000210	0.718322

[a] Calculated from Equation (3), [b] Calculated from Equation (10), [c] Calculated from Equation (11), [d] Calculated from Equation (7)

Table A2. Summary of selected calculated parameters for the 5 g clay and 10 g glass bead membrane at 2500 psi.

Mass (g)	**Time (Hours)**	**[a] Jv (cm/s)**	**[b] L_p (m^3/N-s)**	**[c] $C_{(0,\,t)}$ (M)**	**[d] $C_{(e,\,t)}$(M)**	**[e] σ**	**$C_{(experiment)}$**	**C_{et}/C_i**
	0						0.000303	1
147.435	49.63	2.15×10^{-05}	6.23×10^{-14}	0.000591	0.000222	0.45	0.000116	0.381684
103.170	73.32	3.15×10^{-05}	9.14×10^{-14}	0.000607	0.000256	0.39	0.000285	0.939655
138.550	116.62	2.31×10^{-05}	6.71×10^{-14}	0.000607	0.000263	0.37	0.000274	0.904114
105.290	136.33	3.86×10^{-05}	1.12×10^{-14}	0.000607	0.000281	0.34	0.000290	0.957195
94.390	171.85	1.92×10^{-05}	5.58×10^{-14}	0.000607	0.000270	0.32	0.000271	0.893041
63.100	197.90	1.75×10^{-05}	5.08×10^{-14}	0.000607	0.000272	0.30	0.000259	0.854381
90.770	219.88	2.99×10^{-05}	8.66×10^{-14}	0.000607	0.000285	0.30	0.000231	0.760746
100.995	263.52	1.67×10^{-05}	4.86×10^{-14}	0.000607	0.000278	0.29	0.000238	0.783601
84.320	289.63	2.34×10^{-05}	6.77×10^{-14}	0.000607	0.000286	0.29	0.000202	0.665692
110.085	319.28	2.69×10^{-05}	7.79×10^{-14}	0.000607	0.000289	0.29	0.000223	0.735977
112.010	336.60	4.68×10^{-05}	1.36×10^{-13}	0.000607	0.000295	0.29	0.000298	0.982283
91.960	385.53	1.36×10^{-05}	3.94×10^{-14}	0.000607	0.000282	0.28	0.000333	1.098473
129.195	425.72	2.33×10^{-05}	6.75×10^{-14}	0.000607	0.000291	0.28	0.000322	1.062737
134.295	473.27	2.04×10^{-05}	5.93×10^{-14}	0.000607	0.000291	0.27	0.000322	1.060115
120.825	527.32	1.62×10^{-05}	4.69×10^{-14}	0.000607	0.000290	0.27	0.000343	1.130080

[a] Calculated from Equation (3), [b] Calculated from Equation (10), [c] Calculated from Equation (11), [d] Calculated from Equation (7)

Table A3. Summary of selected calculated parameters for the 5 g clay and 10 g glass bead membrane at 500 psi.

Mass(g)	Time (Hours)	Jv (cm/s)	[b] $C_{(0,t)}$ (M)	[c] $C_{(e,t)}$(M)	[d] σ	$C_{(experiment)}$	$C_{e,t}/C_i$
	0					0.000349	1
99.060	21.65	3.31×10^{-5}	0.000681	0.000213	0.52	0.000260	0.744681
115.880	47.32	3.27×10^{-5}	0.000688	0.000273	0.45	0.000290	0.832377
112.980	73.22	3.15×10^{-5}	0.000685	0.000295	0.40	0.000314	0.900509
97.062	122.90	1.41×10^{-5}	0.000612	0.000295	0.34	0.000287	0.82234
236.987	170.45	3.60×10^{-5}	0.000697	0.000326	0.38	0.000286	0.819149
102.540	193.03	3.28×10^{-5}	0.000682	0.000327	0.31	0.000296	0.847595
129.517	216.32	4.02×10^{-5}	0.000696	0.000332	0.31	0.000329	0.942923
120.520	240.12	3.66×10^{-5}	0.000693	0.000333	0.30	0.000357	1.023959
140.180	264.35	4.18×10^{-5}	0.000697	0.000336	0.31	0.000383	1.097364
135.687	288.25	4.11×10^{-5}	0.000697	0.000337	0.30	0.000281	0.804625
139.591	312.15	4.22×10^{-5}	0.000697	0.000338	0.30	0.000276	0.791489
138.662	336.15	4.18×10^{-5}	0.000697	0.000338	0.29	0.000297	0.85074
126.960	367.45	2.93×10^{-5}	0.000687	0.000336	0.28	0.000279	0.79889
116.790	387.52	4.21×10^{-5}	0.000696	0.000340	0.28	0.000237	0.680204
91.380	408.80	3.11×10^{-5}	0.000671	0.000338	0.27	0.000268	0.768501
126.625	432.33	3.89×10^{-5}	0.000696	0.000340	0.28	0.000285	0.817021
111.820	457.30	3.24×10^{-5}	0.000686	0.000339	0.27	0.000295	0.84667
140.940	483.32	3.92×10^{-5}	0.000697	0.000341	0.27	0.000354	1.016096
119.110	503.68	4.23×10^{-5}	0.000696	0.000342	0.27	0.000355	1.019426
140.698	527.98	4.19×10^{-5}	0.000697	0.000342	0.27	0.000347	0.994773
143.137	552.38	4.24×10^{-5}	0.000697	0.000343	0.27	0.000342	0.981591

[a] Calculated from Equation (3), [b] Calculated from Equation (10), [c] Calculated from Equation (11), [d] Calculated from Equation (7)

Table A4. Summary of selected calculated parameters for the 5 g clay and 10 g glass bead membrane at 4500 psi.

Mass (g)	**Time (Hours)**	**Jv (cm/s)**	**[b] $C_{(0,t)}$ (M)**	**[c] $C_{(e,t)}$(M)**	**[d] σ**	**$C_{(experiment)}$**	**$C_{e,t}/C_i$**
	0					0.000226	1
139.745	24.45	3.46×10^{-5}	0.000448	0.000147	0.18	0.000185	0.81653
246.445	73.6167	3.29×10^{-5}	0.000453	0.000192	0.00	0.000226	0.996544
138.030	97.25	3.52×10^{-5}	0.000453	0.000201	0.12	0.000198	0.875846
216.425	140.567	3.24×10^{-5}	0.000453	0.000207	0.64	0.000081	0.358105
169.745	172.25	3.35×10^{-5}	0.000453	0.000211	0.58	0.000094	0.416352
109.490	195.783	2.64×10^{-5}	0.000453	0.000209	0.52	0.000109	0.479836
113.195	221.517	2.56×10^{-5}	0.000453	0.000211	0.53	0.000107	0.471393
112.050	243.833	2.91×10^{-5}	0.000453	0.000214	0.61	0.000087	0.386249
188.475	311.35	1.78×10^{-5}	0.000453	0.000211	0.88	0.000027	0.117919
135.845	362.85	1.59×10^{-5}	0.000453	0.000212	0.88	0.000027	0.117741
174.200	427.15	1.71×10^{-5}	0.000453	0.000214	0.95	0.000011	0.04731
166.435	523.217	1.09×10^{-5}	0.000453	0.000212	0.00	0.000227	1.00114
142.100	583.617	1.44×10^{-5}	0.000453	0.000216	-0.07	0.000243	1.074421
182.855	626.183	2.73×10^{-5}	0.000453	0.000221	0.10	0.000203	0.895654

[a] Calculated from Equation (3), [b] Calculated from Equation (10), [c] Calculated from Equation (11), [d] Calculated from Equation

Table A5. Mass balance calculations for 5 g clay at 2500 psi.

Samples	**Mass**	**mg/l**	**Nitrate Concentration (M)**	**Total (Nitrate)**
	Influent	18.12	0.000292	
1	141.995	10.42	0.000168	0.02386
2	133.05	10.66	0.000172	0.02287
3	109.72	11.68	0.000188	0.02067
4	184.51	10.81	0.000174	0.03216
5	122.098	9.39	0.000151	0.01849
6	123.52	9.18	0.000148	0.01829
7	214.525	8.90	0.000144	0.03080
8	128.62	12.11	0.000195	0.02512
9	210.445	12.13	0.000196	0.04117
10	129.792	13.34	0.000215	0.02793
11	114.785	13.93	0.000225	0.02578
12	121.57	13.61	0.000220	0.02668
13	134.11	12.31	0.000198	0.02662
14	138.975	14.30	0.000231	0.03205
15	118.34	14.45	0.000233	0.02757
16	136.55	14.59	0.000235	0.03213
17	87.05	14.67	0.000237	0.02060
18	146.74	14.24	0.000230	0.03369
19	94.765	13.82	0.000223	0.02113
20	121.495	13.02	0.000210	0.02551
21	87.43	13.67	0.000221	0.01928
Total	2800.085			0.55242
Total sample volume (ml)	2800.085			
Total Sample Nitrate	0.55242			
Cell volume (ml)	550			
Total influent volume (ml)	3350.085			
Input nitrates (mol)	0.97922			
C_{cell} (M)	0.000382			
Cell Nitrate (mol)	0.21036			

Table A6. Mass balance calculations for 5 g clay and 10 g glass beads at 2500 psi

Sample	**Mass**	**mg/l**	**Nitrate Con (M)**	**Total Nitrate (mol)**
	Influent	18.81	0.000303	
1	147.435	7.18	0.000116	0.01708
2	103.17	17.68	0.000285	0.02942
3	138.55	17.01	0.000274	0.03801
4	105.29	18.01	0.000290	0.03058
5	94.39	16.80	0.000271	0.02558
6	63.1	16.07	0.000259	0.01636
7	90.77	14.31	0.000231	0.02095
8	100.995	14.74	0.000238	0.02402
9	84.32	12.52	0.000202	0.01703
10	110.085	13.85	0.000223	0.02459
11	112.01	18.48	0.000298	0.03339
12	91.96	20.67	0.000333	0.03065
13	129.195	19.99	0.000322	0.04166
14	134.295	19.95	0.000322	0.04320
15	120.825	21.26	0.000343	0.04143
Total	1626.39			0.43396
Total Sample Volume (ml)	1626.39			
Total sample nitrate(mol)	0.43396			
Cell volume (ml)	550			
Total influent volume	2176.39			
Input nitrate	0.66043			
C_{cell} (M)	0.000373			
Cell Nitrate (mol)	0.20517			

Table A7. Mass balance calculations for 5 g clay and 10 g glass beads at 500 psi.

Sample	Mass	mg/l	Nitrate Con (M)	Total Nitrate (mol)
	Influent	20.026	0.000323	
1	99.06	16.10	0.000260	0.02572
2	115.88	18.00	0.000290	0.03364
3	112.98	19.47	0.000314	0.03548
4	97.06	17.78	0.000287	0.02783
5	236.99	17.71	0.000286	0.06769
6	102.54	18.33	0.000296	0.03031
7	129.52	20.39	0.000329	0.04259
8	120.52	22.14	0.000357	0.04303
9	140.18	23.73	0.000383	0.05364
10	135.69	17.40	0.000281	0.03807
11	139.59	17.11	0.000276	0.03853
12	138.66	18.39	0.000297	0.04114
13	126.96	17.27	0.000279	0.03537
14	116.79	14.71	0.000237	0.02770
15	91.38	16.62	0.000268	0.02449
16	126.63	17.66	0.000285	0.03608
17	111.82	18.31	0.000295	0.03301
18	140.94	21.97	0.000354	0.04994
19	119.11	22.04	0.000355	0.04234
20	140.70	21.51	0.000347	0.04881
21	143.14	21.22	0.000342	0.04899
22	133.62	21.42	0.000345	0.04616
23	131.59	21.60	0.000348	0.04585
24	93.89	21.17	0.000342	0.03206
25	130.73	21.33	0.000344	0.04497
26	123.49	21.34	0.000344	0.04251
27	116.99	21.38	0.000345	0.04034
28	139.58	20.58	0.000332	0.04632
29	126.92	21.07	0.000340	0.04314
Total	2788.88			0.90248
Total sample volume (ml)	2788.88			
Total sample nitrate (mol)	0.90248			
Cell volume (ml)	550			
Total influent volume (ml)	3338.88			
Input nitrate (mol)	1.09784			
C_{cell} (M)	0.000333			
Cell Nitrate (mol)	0.18126			